Journal of Photonics for Energy

PhotonicsforEnergy.SPIEDigitalLibrary.org

Transparent electrodes for organic optoelectronic devices: a review

Weiran Cao
Jian Li
Hongzheng Chen
Jiangeng Xue

SPIE.

REVIEW

Transparent electrodes for organic optoelectronic devices: a review

Weiran Cao,[a] Jian Li,[b] Hongzheng Chen,[c] and Jiangeng Xue[a,c,*]
[a]University of Florida, Department of Materials Science and Engineering, Gainesville, Florida 32611, United States
[b]Arizona State University, Department of Material Science and Engineering, Tempe, Arizona 85284, United States
[c]Zhejiang University, Department of Polymer Science and Engineering, Hangzhou, Zhejiang 310058, China

Abstract. Transparent conductive electrodes are one of the essential components for organic optoelectronic devices, including photovoltaic cells and light-emitting diodes. Indium-tin oxide (ITO) is the most common transparent electrode in these devices due to its excellent optical and electrical properties. However, the manufacturing of ITO film requires precious raw materials and expensive processes, which limits their compatibility with mass production of large-area, low-cost devices. The optical/electrical properties of ITO are strongly dependent on the deposition processes and treatment conditions, whereas its brittleness and the potential damage to underlying films during deposition also present challenges for its use in flexible devices. Recently, several other transparent conductive materials, which have various degrees of success relative to commercial applications have been developed to address these issues. Starting from the basic properties of ITO and the effect of various ITO surface modification methods, here we review four different groups of materials, doped metal oxides, thin metals, conducting polymers, and nanomaterials (including carbon nanotubes, graphene, and metal nanowires), that have been reported as transparent electrodes in organic optoelectronic materials. Particular emphasis is given to their optical/electrical and other material properties, deposition techniques, and applications in organic optoelectronic devices. [DOI: 10.1117/1.JPE.4.040990]

Keywords: transparent conductive electrodes; organic optoelectronic device; doped metal oxide; thin metal layer; transparent polymer electrodes; carbon nanotubes; graphene; metal nanowires.

Paper 14040MV received Jun. 16, 2014; revised manuscript received Aug. 21, 2014; accepted for publication Sep. 15, 2014; published online Oct. 30, 2014.

1 Introduction

Optoelectronic devices based on organic semiconductors, including conjugated small molecules and polymers, have attracted tremendous academic and industrial attention, due to the many technological advantages of organic materials, such as low material cost, great diversity, tunable material properties, and compatibility with flexible substrates and low temperature/high throughput manufacturing processes.[1–4] Over the last decade, the performance of optoelectronic devices has rapidly advanced in terms of efficiency and lifetime, especially those of organic photovoltaic (OPV) cells and organic light-emitting diodes (OLEDs). The state-of-the-art power conversion efficiency of OPV devices has exceeded 10%, which is now approaching the proposed industry required efficiency.[5,6] The OLED technology has already reached commercial applications in displays: Samsung's active-matrix OLED displays in smart phones and LG's 55-in. OLED TV are some examples.

As shown in Fig. 1, the basic device architectures of most OPV and OLED devices can be classified into three different groups according to the position of the light transmissive window,

*Address all correspondence to: Jiangeng Xue, jxue@mse.ufl.edu

i.e., the transparent electrode (TE), which allows light into and out of the devices, which also relates to the device fabrication sequence. Most commonly, as shown in Fig. 1(a), a TE is first deposited on a transparent substrate, upon which organic layers and a reflective electrode are subsequently deposited. This configuration corresponds to the superstrate type for OPV devices or the bottom-emitting type for OLEDs, in which light travels through the bottom transparent electrode and the substrate. When the positions of the transparent and reflective electrodes in the devices are switched as shown in Fig. 1(b) such that light travels through the top electrode, we have a substrate type OPV device or a top-emitting OLED. Here, an opaque substrate could be used. In some other cases, transparent (or semitransparent) OPV or OLED devices can be achieved when both electrodes are transparent (or semitransparent) such that light travels through the bottom and top electrodes as shown in Fig. 1(c).

As a TE in optoelectronic devices, optical transparency and electrical conductivity are obviously two key parameters that are related to the device performance. Moreover, the electrode/active layer interfaces, which can strongly influence the device performance, are closely related to various material properties of the electrodes and the deposition methods used. Hence, other properties, such as surface roughness, surface chemistry, work function, processibility, and mechanical properties, are also important factors for evaluating a candidate material for use as the TE in a particular type of device. Some of these parameters are especially important when the transparent electrodes are deposited on top of the organic layers [see Figs. 1(b) and 1(c)]. As organic materials are generally susceptible to high temperature, organic solvents, and ion/atom bombardment, it is more challenging to find suitable top transparent electrodes and related deposition techniques that can eliminate or minimize the damage to underlying active materials.

So far, indium-tin oxide (ITO) has been the material of choice as the TE in most OPV and OLED devices as a result of its excellent optoelectronic properties and environmental stability.[7–9] Commercial ITO thin films usually have sheet resistances of 20 $\Omega/\square$ or less for 100- to 300-nm-thick films (corresponding to conductivity on the order of 10^3 S/cm) and a typical transmittance of >80% in the visible spectral range. Although ITO is the dominant electrode for optoelectronic devices, it still has several drawbacks for large-scale applications.[10–12] First, the rising cost of indium, associated with the scarcity of global indium resources and its large consumption, is one of the greatest concerns for the boosted demand of ITO due to the popularity of liquid crystal displays, solid-state lighting, solar panels, and other products.[13–15] The deposition techniques and surface treatment processes also add to the cost of ITO.[16] Generally, most of the commercialized ITO thin films are deposited by magnetron sputtering, molecular beam epitaxy, thermal evaporation, and pulse laser deposition. All these techniques require high treatment temperatures, 400 to 500°C or higher, and high-vacuum related deposition tools, which further increases the ITO price[17,18] and makes it unsuitable for use as top electrodes in organic optoelectronic

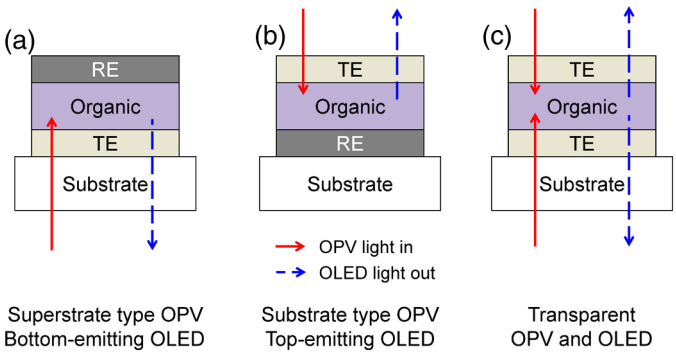

Fig. 1 Schematic illustration of three types of general organic photovoltaic (OPV) and organic light-emitting diode (OLED) device architectures: (a) superstrate type OPV and bottom-emitting OLED, where light transfers into or out of the device through bottom substrates and transparent electrodes; (b) substrate type OPV and top-emitting OLED, where light travels through top transparent electrodes; and (c) transparent OPV and OLED, where light travels through both bottom and top transparent electrodes.

devices or for use with plastic substrates. Furthermore, the inefficient material utilization for these deposition techniques is another factor that increases the cost of ITOs. For example, ~30% of the ITO in the source targets can reach the substrates during the sputter deposition process, and the remaining 70% of the sputtered ITO source material is left on the sidewalls and masks of the sputtering chamber. ITO recycling, either from the deposition process or from the scraped optoelectronic products containing ITO films, has become one of the critical ways to minimize ITO manufacturing costs. Aside from the high cost of raw materials, the high temperature-related deposition processes will damage the underlying organic materials when being utilized as top TEs in OPV and OLED devices. Due to the intrinsic flexibility of organic semiconductors, the next-generation organic optoelectronic devices are envisioned to be fabricated on flexible substrates to realize flexible and lightweight optoelectronic products. However, the high temperature deposition process and the brittle nature of ITO impede its applications in flexible modules. Last but not least, the nonstoichiometry nature of ITO makes its properties very variable and strongly dependent on the processing history (including source material composition, deposition method and conditions, postdeposition handling/treatment).[9]

In the past few years, various alternative transparent conductive materials have been developed to address the above issues of ITO. In this review, we discuss four groups of materials that have been utilized as TEs in organic optoelectronic devices, especially in OPV and OLED devices: doped metal oxides, thin metal layers, transparent conductive polymers, and nanoscale materials [carbon nanotubes (CNTs), graphene, and metal nanowires (NWs)]. High optical transparency in designated spectral regions and low sheet resistance are generally required to achieve high optoelectronic device performance; however, there generally exists a trade-off between these two key parameters. If we neglect any surface or interface effects and assume the material is homogeneous, the sheet resistance of the electrode, R_{Sh}, should scale inversely with its thickness, t, i.e., $R_{\mathrm{sh}} = (\sigma t)^{-1}$, whereas the transparency, T, follows an exponential decay behavior with t as $T = \exp(-\alpha t)$ according to the Beer-Lambert law. Here σ and α are the electrical conductivity and absorption coefficient (which is wavelength dependent), respectively. Hence increasing the electrode thickness leads to lowering in both sheet resistance and transparency. In addition to the thickness dependency, the transparency of these electrodes could have a weak or strong wavelength dependence, and the surface/interface effects (roughness, patterning, optical interference, etc.) as well as material synthesis/processing conditions could also play important roles in determining both transparency and resistance in many cases. The representative transparency (in the visible spectral range) and sheet resistance values of the four groups of transparent conductive materials in optimized (or near-optimized) conditions are summarized in Fig. 2 and Table 1.[11,13,19–53] Table 1 also summarizes some other relevant factors for using these materials as TEs in OPV and OLED devices/modules, which include compatibility

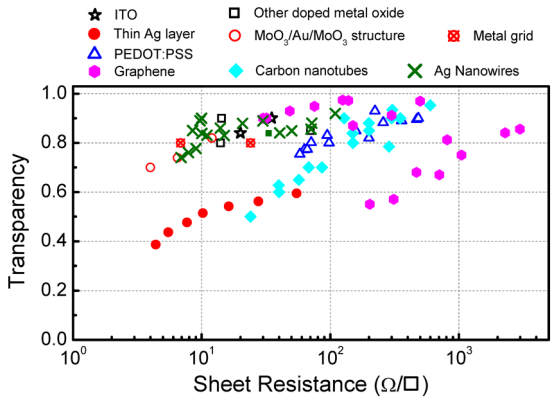

Fig. 2 Literature-reported transparency values in the visible spectral range as a function of the sheet resistance for transparent conductive materials: indium-tin oxide (ITO),[22,35] other doped metal oxides,[21,33] thin metal layers,[29,34,41,46] dielectric/metal/dielectric multilayers,[44] metal grids,[23,52] poly(3,4-ethylene dioxythiophene):polystyrene sulfonic acid layers,[13,15,36,37,45,48,51] graphene,[28,29,31,32,47] carbon nanotube films,[19,20,26,30,43,45,53] and Ag nanowires.[11,29,39,40,42,50]

Table 1 List of representative key parameters of different types of transparent conductive materials for use as transparent electrodes in organic optoelectronic devices.

Type	Material	Transparency[a] (%)	Sheet resistance[a] (Ω/□)	Compatibility with flexible substrate	Use as top electrode	Stability
Doped metal oxide	Indium-tin oxide	80 to 95	10 to 50	No	Difficult (sputtering damage, high temperature process)	Good
	ZnO:Al	80 to 95	10 to 100	No	Difficult (sputtering damage, high temperature process)	Poor stability when they are ultrathin[24]
Thin metal layer	Thin metal layers	40 to 60	1 to 80	Yes	Yes	Depend on metal material
	Dielectric/metal/dielectric multilayers	70 to 85	1 to 80	Yes	Yes	Unknown
	Metal grids	~80	6 to 50	Yes	Difficult (patterning issue)	Unknown
Transparent conductive polymer	Poly(3,4-ethylene dioxythiophene): polystyrene sulfonic acid	75 to 90	50 to 1000	Yes	Yes	Degrade under humidity, high temperature, and UV exposure[25,27]
Nanoscale material	Graphene	60 to 95 90, 97.4[47]	100 to 3000 30, 125[47]	Yes	Difficult (complicated process)	Unknown
	Carbon nanotube	50 to 95	20 to 1000	Yes	Difficult (complicated process)	Unknown
	Ag nanowire	70 to 90	5 to 200	Yes	Yes	Corrode through chemical reaction, such as oxidation and suffixation[38,49]

[a]Transparency and sheet resistance values are obtained from the same references as listed in Fig. 2.

with flexible substrates and large-scale processes, the possibility of using them as top TEs, and their environmental stability.

In the following sections, we will review the basic material/film properties for all four groups of materials in detail, along with their compatibility with large-scale and low-cost fabrication methods. We will also review their applications in OPV and OLED devices, and will especially compare the device performance and device flexibility based on these alternatives with ITO-reference devices then discuss their possibility as top TEs.

2 Transparent Conductive Oxides

Doped metal oxides are the most common transparent conductive oxide layers in organic optoelectronic devices. Doped metal oxide thin films are usually highly transparent (>80% transmittance) due to the wide bandgap of most metal oxides, while the doped elements can generate oxygen vacancies, interstitial defects, and doped metal ions that assist the charge carrier transport and enable the high conductivity of oxide films.[54,55] As mentioned above, ITO is the most widely used TE material in OPV and OLED devices with its excellent electronic conductivity and optical

transparency in the visible light range. In most OPV and OLED devices, ITO is usually deposited on transparent substrates as the bottom electrode and light window; therefore, the physical properties of ITO films, including the surface roughness, film conductivity, work function, etc., strongly affect the device performance. Extensive work has been carried out to modify the ITO surface with various treatments, such as mechanical polishing, ion-beam sputtering, oxygen plasma, and UV-ozone or chemical treatments.[9,56,57]

The work function (WF) of an electrode plays a critical role in determining the carrier (electron or hole) injection barrier height into the active materials. The WF of as-received ITO films is typically in the range from 4.3 to 4.7 eV, which is neither close to the lowest unoccupied molecular orbital (LUMO) level nor to the highest occupied molecular orbital level of most organic semiconductors used in OLED and OPV devices. Hence, the nonzero potential barrier for the hole or electron states between the ITO electrodes and organic layers may present a critical limit on the charge collection/injection efficiency for OPV and OLED devices.[58–60] Several surface treatments have been demonstrated to modify the work function for achieving a better device performance. UV-ozone and O_2 plasma treatment are the most simple and widely used methods to increase the work function of ITO films, normally up to 4.7 to 5.0 eV, which is generally attributed to the incorporation of oxygen onto the ITO electrode surface.[61,62] The solution casted poly(3,4-ethylene dioxythiophene):polystyrene sulfonic acid (PEDOT:PSS) layer (WF $\approx$ 5.1 eV) is the most popular anode modification layer for OPV and OLED devices with ITO as anodes.[63,64] Alternatively, some transparent transition metal oxide thin films have been demonstrated as good buffer layers between ITO and organic layers. Normally, MoO_x, NiO, and WO_x are hole-selective materials in optoelectronic devices and are used as anode modification materials,[65–68] whereas ZnO and TiO_x are electron-selective layers that allow efficient electron collection and injection.[69–73] Self-assembling a monolayer of organic molecules on the ITO surface has emerged as another effective routine to modify the electronic and chemical properties of the ITO surface and engineer the ITO/organic interfaces. In general, one end of these self-assembled molecules can spontaneously form tight bonds with the surface atoms of ITO, whereas the other end of the molecular chain can be functionalized with polar groups. The dipole moments of these molecules will affect the vacuum level outside the ITO electrode and vary its effective work function.[74–77] Recently, Helander et al. reported another novel method to significantly increase the ITO work function by functionalizing the ITO surface with a monolayer of chlorine [named chlorinated ITO (Cl-ITO)]. With a controllable number of electron-negative halogen atoms anchored on ITO surface, the ITO work function can be tuned from 4.7 eV to a maximum value of WF = 6.13 eV.[78] Helander et al. also demonstrated phosphorescent OLED devices with the Cl-ITO anodes, where the high ITO work function matched with the LUMO level of the host material, 4,4′-N,N′- dicarbazole-biphenyl, and enabled the direct injection of holes from ITO to the host. Therefore, the OLED device structure was simplified with no hole injection and transport layers and the device efficiency was greatly improved with less charge transport barriers and exciton quenching interfaces.[78]

Magnetron sputtering, molecular beam epitaxy, thermal evaporation, pulse laser deposition, etc., are the major deposition techniques for achieving high-quality ITO films. Normally, these techniques are suitable for ITO deposition on hard substrates that can withstand high temperature processing as bottom electrodes in OPV and OLED devices; however, the high-energy ions or atoms along with possible heat and radiations during these deposition processes may cause significant damage to the underlying organic films, thus limiting the application of ITO electrodes as top electrodes in organic-based optoelectronic devices.[79,80] For example, sputtering ITO without specifically heating the substrate often leads to lower electrical conductivity and/or lower optical transparency than in commercially available ITO electrodes on glass substrates, which generally require high substrate temperatures during deposition or high temperature postdeposition annealing.[9] When using ITO as the top electrode, it is desirable to use some buffer layers or sacrificial layers, such as organic protective layers [e.g., copper phthalocyanine (CuPc) layer],[81] thin metal layers (e.g., Mg/Ag layer),[82] or some transition metal oxide layers (e.g., MoO_x),[83] to protect the underlying organic active layer during ITO deposition, without negatively affecting the charge injection/transport characteristics of the device. Low-energy magnetron sputtering methods have also been developed to reduce the damages to organic layers.[84–86] There have

been several successes in demonstrating OPV and OLED devices with sputtered top ITO electrodes; however, the optical and electronic properties for these ITO films with low energy deposition techniques are quite different from commercial ITO electrodes in addition to a very slow deposition process with film growth rates as low as 0.1 Å/s,[9,87] which need to be further studied and improved for their large-scale applications.

Furthermore, the poor mechanical properties of ITO layers are another issue that affects their application in flexible and portable electronic products. As reported in previous literature, microcracks were observed in ITO thin layers after repeated flexing and large angle bending, leading to a dramatic decrease in film conductance as well as device performance.[44,48,88] Though there are companies and research groups working on methods to engineer the ITO film quality, such as varying the deposition methods and modifying the indium to tin ratio, it is still a great challenge to fully solve this problem.

Zinc oxide (ZnO), which has a wide bandgap (>3 eV) and is transparent in the visible spectral range, is one of the attractive ITO alternates due to the abundant material storage and its environmental nontoxicity. Similar to that of ITO, some extrinsic dopants, such as Al and Ga, are added into the ZnO films to improve the film conductivity by introducing ionic impurities.[33,45,89] Hence, these Al-doped ZnO (AZO)[33,90,91] and Ga-doped ZnO (GZO)[21,92] films show comparable optical transparency and electrical conductivity as the ITO layers and have been developed as TEs in optoelectronic devices. AZO and GZO have a work function range of 4.0 to 5.0 eV depending on the surface treatments.[93,94] By selecting suitable interlayers as those described for ITO modification, they can serve as either anodes or cathodes in OPV and OLED cells. For example, Liu et al. reported an ~850-nm-thick-thick AZO electrode with a sheet resistance of ~14 Ω/□ and a transparency of ~80% in the visage spectral range. An ITO-free inverted poly[[4,8-bis[(2-ethylhexyl)oxy]benzo-[1,2-b:4,5-*b′*]dithiophene-2,6-diyl][3-fluoro-2-[(2-ethylhexyl)-carbonyl]-thieno-[3,4-*b*]-thiophenediyl]]:[6,6]-phenyl-C_{71}-butyric acid methyl ester OPV device was successfully demonstrated with such an AZO TE, which showed an optimized power conversion efficiency (η_P) of 6.15%, only slightly lower than the ITO-based devices ($\eta_P = 6.57\%$).[91] Other than AZO and GZO, many other doped metal oxides have been investigated and utilized as TEs in optoelectronic devices. For example, fluorine-doped tin oxide is another type of the doped metal oxide electrodes that are widely used as electron collection electrodes in dye sensitized solar cells.[95,96] Most recently, they have also been broadly used as bottom transparent cathodes in inverted planar heterojunction solar cells due to the rapidly developing new photovoltaic active materials, perovskites, with a power conversion efficiency of >15%.[96–98]

Though the material-related cost for these doped metal oxide is reduced by getting rid of the scarce materials, similar costly deposition techniques, such as sputter, chemical vapor deposition, atomic layer deposition, and pulse laser deposition, are still required for achieving high-quality films for such indium-free materials.[89,99] More efforts are required to develop cheaper processing methods (e.g., solution-process) to reduce the overall cost for TE fabrication. As ceramics, they also have poor mechanical properties like ITO, which is not compatible with flexible substrates and high-throughput roll-to-roll processes. Additionally, some reports have shown that some of these materials like AZO have poor environmental stability when they are ultrathin (<100 nm), further limiting their applications in optoelectronic devices.[24]

3 Metal-Based (Semi-)Transparent Electrodes

While thick metal layers (e.g., Al and Ag), with thicknesses on the order of 100 nm, have been widely used as reflecting electrodes in most optoelectronic devices, ultrathin metal layers (normally <20 nm thick) are semitransparent to visible light due to the skin depth of the electromagnetic wave for these metals. Such ultrathin metal layers have emerged as a potential ITO substitute in optoelectronic devices in laboratories.[100–104] Significant effort has been made to improve the transparency of ultrathin metal layers while maintaining their high conductivity.[105] In this section, we will discuss the application of thin metal layers, dielectric/metal/dielectric multilayer structures, and metal grids for improved transparency as TEs in OPV and OLED devices.

3.1 *Ultrathin Metal Layers*

There is a trade-off between the transparency and conductivity for ultrathin metal layers. Though a sufficiently thin metal layer allows most of the light to be transmitted (high transparency), the discontinuity in film morphology results in poor electrical conductivity for ultrathin metal films.[41,106,107] Wilken et al. measured the sheet resistance of Au thin films on glass substrates with different nominal film thicknesses (from 10 to 60 nm). As shown in Fig. 3(a), while the experimental data (open symbols) qualitatively follow the predicted trend from the Fuchs-Sondheimer and Mayadas-Shatzkes models based on the scattering of free charge carriers,[104] the Au films with thicknesses >20 nm have low sheet resistances of <5 $\Omega/\square$; however, the sheet resistance dramatically increases to >50 $\Omega/\square$ for films <10 nm. Shown in the inset of Fig. 3(a) is a comparison of transmittance of the Au films with different thicknesses. A maximum transmittance of ~70% at $\lambda = 500$ nm was obtained for a 7-nm-thick Au film, which was reduced to <60% for a 12-nm-thick film. In addition, the transmittance exhibits strong wavelength dependence. For example, the transmittance is only 50% at $\lambda = 700$ nm compared to the peak of 70% at $\lambda = 500$ nm for the 7-nm-thick Au film.

With a 9-nm-thick Ag layer as the bottom TE, O'Connor et al. successfully demonstrated a $CuPc/C_{60}$ bilayer OPV device, which exhibited a similar PV performance to that with an ITO electrode [Fig. 3(b)].[103] Although there have been a few studies aimed toward increasing the electrical conductivity without sacrificing the optical transparency,[46,108,109] such as applying a seed layer to improve the continuity of thin metal layers,[110] the relatively low optical transparency of thin metals is still one of the limitations in achieving high-performance devices with them.[111,112]

3.2 *Dielectric/Thin-Metal/Dielectric Electrodes*

Since the first report by Fan et al. in 1974,[113] dielectric/thin-metal/dielectric (DMD) multilayer structures have been extensively studied for achieving highly transparent and conductive electrodes.[114–117] In these DMD electrodes, the intermediate thin metal layer provides the electrical conductance for the entire structure, whereas the two dielectric layers improve the overall transparency due to optical interference within the multilayer structure and the surface plasmonic effects at the two metal/dielectric interfaces.[44,118–120] As shown in Figs. 4(b) and 4(c), an $MoO_x/Au/MoO_x$ structure shows a maximum transmittance of $T = 80\%$ at $\lambda = 650$ nm (the corresponding reflectance is $R = 5\%$), which is about two times higher than that of the bare Au layer ($T = 40\%$ and $R = 25\%$). These experimental results qualitatively agree with

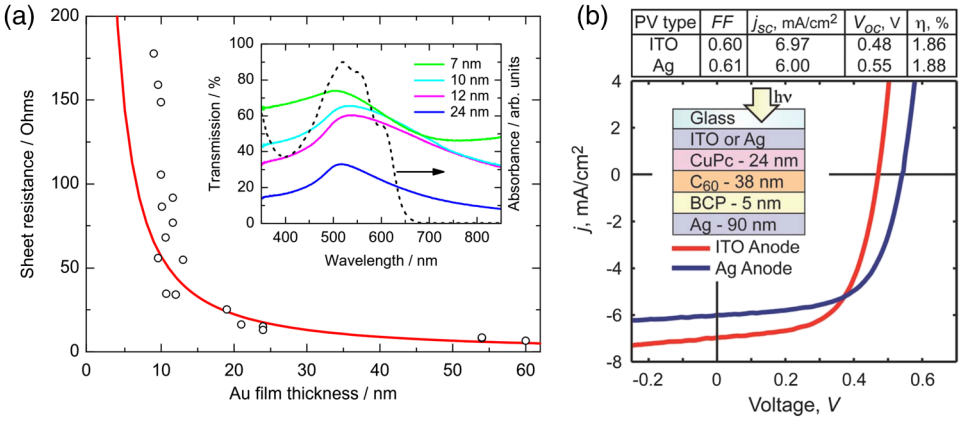

Fig. 3 (a) Sheet resistance of ultrathin Au films with various thicknesses (open dots are experimental results and solid lines are the prediction based on Fuchs-Sondheimer and Mayadas-Shatzkes mode). Inset: Transmittance of Au films with differet thicknesses. Reprinted with permission from Ref. 104. Copyright 2012 Elsevier. (b) A comparison of J – V characteristics of CuPc/C60 devices with ITO and Ag thin films as bottom transparent electrodes. Reprinted with permission from Ref. 103. Copyright 2008 AIP Publishing LLC.

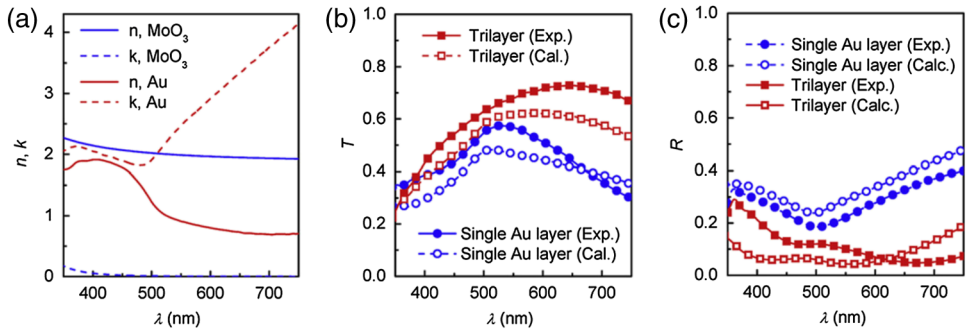

Fig. 4 (a) Optical constants of thin layers of MoO_x and Au for transfer-matix simulations. (b) Comparison of the transmittance of MoO_x/Au/MoO_x trilayer electrode and a 15-nm-thick Au thin layers. (c) Comparison of the reflectance of the trilayer and Au thin layers, where solid symbols are experimental results and open symbols are calculated results. Reprinted with permission from Ref. 44. Copyright 2012 Elsevier.

the calculated transmittance and reflectance [open symbols in Fig. 4(b)] based on the transfer-matrix model with the optical constants listed in Fig. 4(a), which further confirms the transparency enhancement of the DMD structure as a result of the strong optical interference effects within the multilayer structure.[44] In addition to MoO_x,[115,121] other choices for the dielectric layers include metal oxides (ZnO,[122] WO_3,[123,124] etc.), metal sulfides [e.g., ZnS (Refs. 125 and 126], and organic materials (bathocuproine).[127] For example, Cho et al. applied the ZnS/Ag/WO_3 electrode in OLEDs with tris(8-hydroxyquinolinato) aluminum (Alq_3) active layers, which exhibited near-Lambertian emission with comparable current efficiency to ITO-based reference devices.[125] The inner dielectric layer in these DMD electrodes determines the carrier injection/collection polarity of the whole structure. Other than the rare and noble metal materials (e.g., Au and Ag), some other metals, such as Al and Cu, have also been utilized in the electrodes without affecting their electrical properties, which can further reduce the material cost for the entire structure.[128] All the layers in the DMD structures are deposited by low-temperature deposition techniques, such as thermal vacuum deposition and spin coating; hence, these DMD electrodes can be utilized as top TEs with negligible damage to the underlying organic layers.[115,116,129] Wrzesniewski et al. successfully demonstrated a top-emitting OLED (TE-OLED) with a thermal evaporated MoO_x/Au/MoO_x trilayer structure as the top TE, which enabled a very high light extraction efficiency.[116] With transparent and close-packed microlens arrays attached to the DMD electrode, the light extraction efficiency as well as the external quantum efficiency of such TE-OLED devices was increased by up to 2.6 times compared to the ones without the microlens arrays.[116]

Furthermore, such DMD multilayer electrodes show excellent mechanical flexibility in comparison to ITO electrodes because of the good ductility of metal layers, enabling their application in flexible optoelectronic devices.[122] Cao et al. successfully demonstrated a flexible poly(3-hexylthiophene):phenyl-C_{61}-butyric acid methyl ester (P3HT:PCBM) device with MoO_x/Au/MoO_x electrodes on poly(ethylene terephthalate) (PET) substrates [Fig. 5(a)], which shows a nearly identical photovoltaic performance as the similar device fabricated on a glass substrate [Fig. 5(b)]. Cao et al. further studied the mechanical flexibility of the flexible device using a simple bending test method.[44] Only an ~6% drop in efficiency was observed after bending the device 500 times with a bending radius of 1.3 cm [Fig. 5(c)], which is far better than ITO electrodes, which can only sustain a few bending cycles with large bending angles.[44]

In summary, the multilayer structure with a thin metal layer sandwiched between two dielectric layers shows a similar electrical conductivity but an enhanced optical transparency compared to the metal-only semitransparent electrodes. With some advantages over ITO electrodes, such as better flexibility in flexible devices and less damage to organic layers when used as top TEs, these multilayer electrodes have been investigated as potential ITO substitutes. So far, sputter and thermal evaporation are the two major deposition methods for metal and dielectric layers in these DMD electrodes. Achieving the desired thickness for each layer in DMD structures may

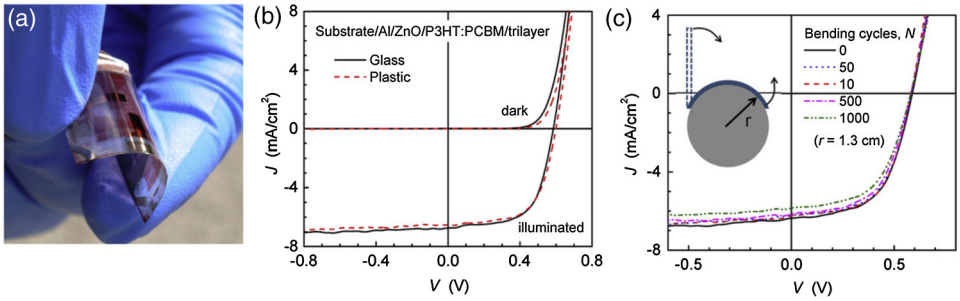

Fig. 5 (a) A photograph of a flexible poly(3-hexylthiophene):phenyl-C61-butyric acid methyl ester (P3HT:PCBM) device with an $MoO_x/Au/MoO_x$ transparent electrode. (b) A comparison of J – V characteristics of P3HT:PCBM devices on glass and plastic substrates. (c) J – V characteristics of devices under different bending conditions. Reprinted with permission from Ref. 44. Copyright 2012 Elsevier.

present some cost issues for fabricating low-cost optoelectronic devices.[130] Moreover, transparency and conductivity of the DMD layers are strongly dependent on the thickness of the multiple thin layers, especially the intermediate metal layer, which is only ~10 nm thick. Therefore, the uniformity of these ultrathin layers is vitally important for optimal properties; better deposition methods are required to make them compatible with large-area OPV and OLED modules.

3.3 *Metal Grids*

Macroscopic metal grids have been widely utilized as the front contact in many inorganic-based solar cells, such as silicon solar cells and copper indium gallium selenide photovoltaic cells, where the metal fingers conduct away the generated current and the openings between the figures become the light windows for light absorption.[131,132] Here, microscopic metal grids composed of ordered metal lines that are <1 μm wide are discussed and considered as a potential replacement for semitransparent continuous metal films for use as TEs in organic optoelectronic devices.[133–135] One of the advantages of metal grids is the increased transparency compared to continuous metal layers, where the gaps between metal lines are blank (100% in transparency) and contribute to the high transparency. The transmittance of metal grids is determined by the percentage of the blank areas on the film, which is related to the metal line width, spacing between lines, and the number of total lines within a unit area. The low sheet resistance of the metal grids can be achieved by using thick metal lines, 100 nm or even thicker, although this comes at the expense of film planarity.[52] However, the openings in the metal grids result in poor electrical contact with the organic materials, which typically have very low conductivity, thus leading to very inefficient charge injection and/or collection at the electrode/organic interface. Generally, a continuous conductive buffer layer (e.g., PEDOT:PSS) is required to planarize the surface of the metal grids and improve electrode contact with the active materials when used in optoelectronic devices.[136]

Conventional photolithography has been one of the predominant patterning methods used to fabricate such ordered metal grids, although it is somewhat complicated, costly, and incompatible with flexible substrates.[137,138] In 2007, Kang and Guo demonstrated a nanoimprint lithography (NIL) technique to achieve these electrodes on both rigid and flexible substrates.[139,140] As schematically illustrated in Fig. 6(a), a soft mold (e.g., polydimethylsiloxane) is first created with the replication of desired features from a hard template patterned using conventional photolithography. The soft mold is a reusable transfer media or stamp which transfers a thin metal layer deposited on its surface to the substrates by applying proper pressure and heat.[139,141] Different metal grids, such as Au, Cu, and Ag, have been successfully fabricated with this NIL method.[23] These printed grids with 70-nm line width and 700 nm periods [Fig. 6(b)] showed an average transmittance of 84, 83, and 78% in the visible spectral range and sheet resistances of 24, 28, and 23 $\Omega/\square$ for Au, Cu, and Ag electrodes, respectively [Fig. 6(c)]. With these metal grids as TEs, both ITO-free OPVs and OLEDs were successfully demonstrated with comparable device performance as the ITO-reference cells.[136,137,140,142] For example, an η_P of ~2.0% was achieved

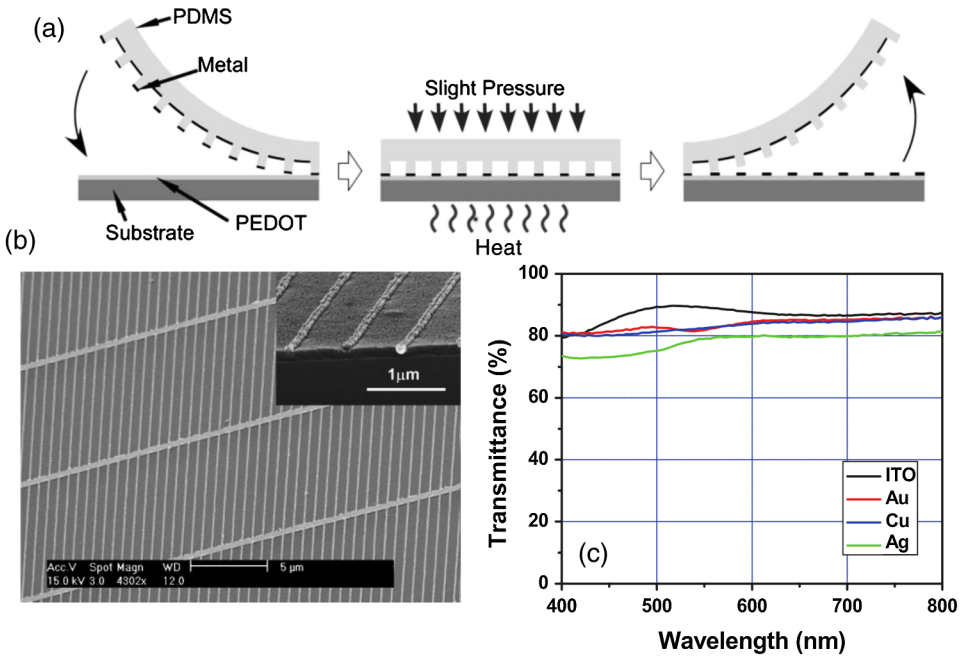

Fig. 6 (a) Schematic illustration of a nanoimprint lithography (NIL) technique to produce metal grids. (b) SEM images of Cu grids fabricated by the NIL method. (c) Optical transmittance of Au, Cu, and Ag grid electrodes and a conventional ITO electrode. Reprinted with permission from Ref. 23. Copyright 2008 John Wiley and Sons.

by using the above metal grids as the transparent anodes in P3HT:PCBM devices, which is comparable to the ITO-based devices fabricated under the same conditions.[23]

Although the development of the NIL technique presents a great opportunity for using metal grids as TEs in electronic devices, there are still several factors that influence the large-scale applications. The extremely rough surfaces (generally in the range of tens of nanometers) limit their application in devices with thin organic layers. It is also difficult to use such metal grids as top TEs in OPVs and OLEDs since the transfer processes (heat or pressure) may cause damage to the underlying organic layers. Moreover, more effort is needed to integrate the NIL techniques with roll-to-roll processing, which is another significant challenge for utilizing metal grids as TEs in large-scale devices.

4 Polymeric Transparent Conductors

Due to the high transparency, easy solution processability, and good compatibility with flexible applications, transparent conductive polymers have also been investigated as alternative low-cost TEs.[12,17,36,143,144] To achieve high electrical conductivities, some conductive polymers, such as polyaniline, polypyrrole, and polythiophene, have been developed with the addition of suitable chemical dopants. Among these, PEDOT:PSS is one of the most successful and widely used conducting polymers for optoelectronic applications, especially for those in organic-based devices.[37,51,145]

Since its discovery in the 1990s, PEDOT:PSS has been widely used as an interlayer in organic-based electronic devices, such as polymer PVs and LEDs, to reduce the ITO roughness and facilitate the hole collection/injection between the polymers and the ITO.[146] Low conductivity PEDOT:PSS was first developed with a conductivity of 1 to 10 S/cm, about three orders of magnitude lower than that of ITO (>4000 S/cm). While the electrical conductivity is not the most critical factor for a thin interlayer between ITO and organic active layer(s), the relatively high resistivity of PEDOT:PSS severely limits its application as a stand-alone electrode. Several methods have been successfully developed to improve the electrical conductivity of commercialized PEDOT:PSS. Some polar organic molecules with a high boiling temperature, such

as dimethylsulfoxide (DMSO),[13,147,148] ethylene glycol (EG),[149,150] diethylene glycol,[151] and sorbitol,[17,152] have been mixed into the PEDOT:PSS aqueous solutions, which can enhance the film conductivity by more than one order of magnitude without affecting the transparency and high work function. For example, Na et al. reported highly conductive PEDOT:PSS layers with an average conductivity of ~470 S/cm by adding 5% DMSO to Baytron PH500 solution, compared to a film conductivity of <1 S/cm without DMSO.[13] Using such a modified PEDOT:PSS layer to replace the bottom ITO electrode, the ITO-free P3HT:PCBM device showed an open-circuit voltage (V_{oc}) of 0.63 V, short-circuit current density (J_{sc}) of 9.73 mA/cm^2, fill factor (FF) of 53.5%, and η_P of 3.27% under 1 sun simulated AM1.5 solar illumination, which was comparable with the ITO-based reference cell ($\eta_P = 3.66\%$) [see Fig. 7(a)]. The authors also explored the flexibility of the PEDOT:PSS films and its based device on PET substrates: as shown in Fig. 7(b), the resistance of the PEDOT:PSS film on a PET substrate remained nearly constant after 2500 bending cycles, while the resistance of conventional ITO films on PET substrate increased >10 times after the bending, which led to a dramatic degradation in device efficiency. The ITO-based cell almost completely degraded after 75 cycles of bending, while the PEDOT:PSS-based devices showed nearly the same efficiency after 300 bending cycles.[13] Similarly, flexible OLEDs with PEDOT:PSS as the anodes have been reported by several research groups.[12,153,154] Wang et al. successfully demonstrated a flexible white OLED using a PEDOT:PSS anode with good device performance (power efficiency of 10.8 lm/W at the brightness of 1000 cd/m^2 was achieved) and mechanical flexibility (power efficiency reached 5.0 lm/W after 100 bending cycles).[155] Some other techniques have also been demonstrated to further increase the PEDOT:PSS film conductivity. Kim et al. reported conductivities of >700 S/cm for PEDOT:PSS films with the addition of 6 vol% EG, which were further increased to 1418 S/cm with solvent post-treatment (immerse the PEDOT:PSS films into EG and dry afterward).[37] Formic acid was also used to treat PEDOT:PSS for high conductivities: the highest conductivity of up to 2050 S/m was successfully achieved with the formic acid treatment, approaching that of ITO.[156] According to these reports, the OPV cells based on the highly conductive PEDOT:PSS TEs exhibited the same efficiency as their ITO counterparts, which suggests their promising applications in optoelectronic devices.

Furthermore, polymer electrodes can be utilized as the top TEs in OPV cells, either deposited directly onto the organic active materials using solution processing, such as spin coating, spray, or ink-jet printing, or indirectly using a stamp-transfer lamination process.[15,148,157–160] Gupta et al. applied a high conductivity PEDOT:PSS layer as a top TE in OPVs using a stamp-transfer method. Top-illuminated P3HT:PCBM devices were successfully fabricated on glass and opaque stainless steel substrates, which had maximum η_P of 2.1 and 3.1% for normal and inverted polarity configurations, respectively.[15] For direct solution deposition, it is important to improve the wetting of the aqueous PEDOT:PSS solution on organic materials, which are typically

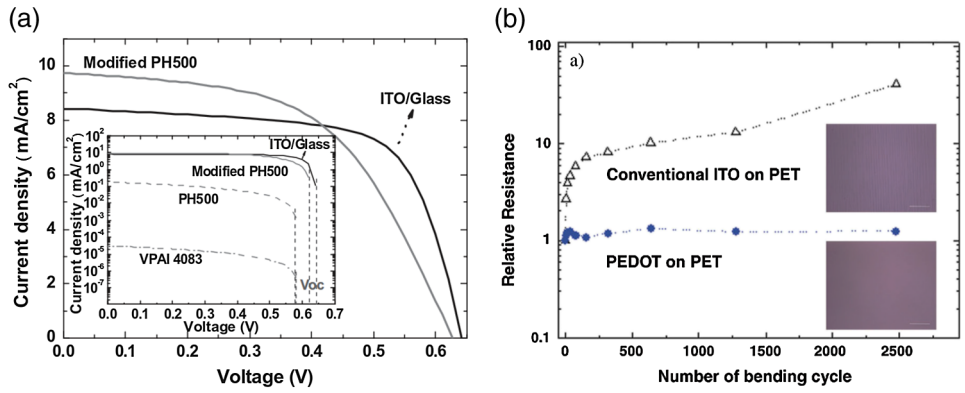

Fig. 7 (a) J – V characteristics of P3HT:PCBM devices with modified PH500 and ITO transparent electrodes. Insert: J – V characteristics of P3HT:PCBM devices with four different anodes: VPAL4083, PH500, modified PH500, and ITO. (b) Relative resistance of ITO and PEDOT:PSS films on PET substrates as a function of number of bending cycles. Reprinted with permission from Ref. 13. Copyright 2008 John Wiley and Sons.

hydrophobic. Several methods have been developed to solve this problem.[48,143,161] For example, Hau et al. demonstrated uniform PEDOT:PSS top electrodes on P3HT:PCBM active layers from diluted PEDOT:PSS solutions with isopropyl alcohol and n-butyl alcohol.[143,162] Some fluorosurfactants, such as Zonyl-FS300, are also used as additives to improve the wetting property of PEDOT:PSS solutions on organic films, which have negligible effects on the electrical and optical properties of PEDOT:PSS films but enables their deposition on most hydrophobic surfaces.[48,163,164]

In summary, transparent polymers, especially the highly conductive PEDOT:PSS, are possible ITO substitutes for TEs, due to their high flexibility and excellent compatibility with large-area, solution-processed coating techniques.[12,165,166] The conductivity of PEDOT:PSS film is approaching that of ITO in certain cases, but further improvement may still be needed, especially when used in large-size, commercial scale devices. Other than doping, *in situ* polymerization of EDOT without adding in PSS components that significantly increase the film conductivity is one other possible method to reduce the PEDOT layer resistance.[152,167–170] Although there have been only a few reported examples on this topic, these attempts open up new routes to improve the electrical properties of polymer electrodes. Moreover, these polymers are known to degrade under humidity, high temperature, and UV exposure.[25,27] Last but not least, the environmental and operational stability of polymer TEs and their related devices must be improved before their extensive usage.

5 Nanomaterials as Transparent Electrodes

Nanoscale materials have been widely studied in the past 20 years in terms of their controllable synthesis and attractive applications in many areas. Some nanomaterials are also being investigated as TEs, such as CNTs, graphene, and metal NWs. The attractive optoelectronic properties of these materials, combined with their high compatibility with solution-processed and large-scale manufacturing, make them very promising candidates as transparent conductive electrodes.

5.1 *Carbon Nanotubes*

Since the first report on CNTs in the early 1990s by Iijima,[171] CNTs have attracted extensive academic and industrial attention due to their unique and promising mechanical and electrical properties. Individual single-walled CNTs (SWCNTs) have charge mobilities of 10^5 cm^2/Vs and electrical conductivities in the 1 to 3×10^6 S/m range.[10,172] Despite the excellent electrical properties of individual tubes, thin films with a network of CNTs show more than three orders of magnitude lower conductivity and mobility (the highest reported conductivity was $\sim$6000 S/m and mobility was $\sim$10 cm^2/Vs) as a result of the large contact resistance between two CNTs.[10] Since the early 2000 s, there have been extensive discussions regarding the potential applications of CNTs as TEs in optoelectronic devices;[173–175] however, several impediments including CNT synthesis, purification, and film processes have hindered their commercial use.

Solution processibility is one of the great advantages for nanoscale materials, which can be integrated with fast, large-scale, and high-throughput manufacturing methods. Therefore, dispersing the CNTs in compatible solvents or obtaining printable inks of CNTs is required for most solution-based deposition techniques.[176] Several studies have shown that unfunctionalized CNTs can be dispersed in some organic solvents, such as chloroform, dichlorobenzene, dimethylformamide, and cyclohexylpyrrolidone. However, the concentration of these CNT solutions has only reached 0.1 to 2 mg/mL, which limits their application for large-scale manufacturing.[176–179] Some dispersion agents or surfactants have been utilized to better promote the suspension of CNTs in organic solvents or even some aqueous media.[180–184] However, most surfactants in CNT solutions become impurities after forming solid films, leading to a significant decrease in film conductivity.[185] Some research groups have demonstrated that it is possible to achieve high concentration and well-dispersed CNT solutions by chemically modifying the CNT surface with covalently bonded functional groups.[176,186] Though such chemical modification assists the dispersion of CNTs and prevents the possible rebundling mechanisms, the anchored small molecules break up the ordered sp^2 bonding structures and become defects in single CNTs, affecting the conductivity of films made from these solutions. Therefore, it is necessary to deeply

understand the relationship between conductivity, surfactants, and molecular structures, which will provide guidance for achieving stable CNT solutions with controllable concentrations while maintaining the good electrical properties of single CNTs and CNT films.

Several solution process techniques, including spin coating,[187,188] spray coating,[30,189] dip coating,[190] and solution-related soft lithography methods,[191–193] have been demonstrated to fabricate uniform transparent conductive CNT films. For example, Wu et al. reported a simple filtration technique to deposit uniform SWCNT films on various substrates. An SWCNT film was first vacuum-filtered on a filtration membrane from a dilute suspension of nanotubes, followed by purification processes to remove possible surfactants and impurities. The SWCNT film was then transferred onto any required substrates after dissolving the membrane in solvent. Benefiting from the vacuum filtration process, this method can provide homogeneous SWCNT films with precisely controllable thicknesses by varying the solution concentration and volume.[174] However, these deposition techniques are only effective for producing films on small area substrates and there are still many challenges to develop cheap and fast deposition techniques for large-scale and uniform CNT films.[194,195]

Besides the processing challenges, the rough surfaces of CNT films combined with the high sheet resistance (>200 Ω/□) as a result of the possible defects and the poor interconnection between CNTs limit their applications in optoelectronic devices. In early reports, OPV devices with CNT films as TEs had η_P of only <1%, compared to 3 to 5% in standard ITO-based devices.[19,196] Many film treatment methods were developed for achieving CNT electrodes with higher electrical conductivity and smoother film surface.[20,26,30,197,198] Tenent et al. reported uniform SWCNT films by using an ultrasonic spray method [see the photograph in Fig. 8(a)] with the sheet resistance of ~150 Ω/□, which was reduced to <50 Ω/□ after nitric acid treatment. As shown in Fig. 8(b), an η_P of 3.1% was achieved for a P3HT:PCBM device with the CNT electrode, which was only slightly lower than the ITO-based cells ($\eta_P = 3.6\%$).[189] Ou et al. demonstrated surface-modified nanotube films with a surface roughness <6.0 nm and sheet resistance of ~100 Ω/□ using PEDOT:PSS modification, HNO_3 acid soaking, and polymer coating. With the modified CNT anodes, a maximum current efficiency of ~10 cd/A was achieved for an Alq3-based OLED, similar to the ITO-based reference devices.[199]

Although there are a few laboratory demonstrations using CNT networks as TEs in OPVs and OLEDs, it is still a long journey for their application in large-scale optoelectronic modules. First, achieving high-quality and low-cost CNTs over a large scale has been one of the challenges in the past 20 years, and will continue to be the research focus of this field in the future.[173] Though some scale-up technologies have been demonstrated by different research groups that have the potential for CNT mass productions, complicated purification processes, such as routes to remove remained impurities after synthesis and methods to distinguish the semiconducting and metallic components, still impede the scalability of high-quality CNTs and, hence, a reduction of the cost.[200,201] In terms of CNT thin films, the relatively low conductivity and transparency are still the two major factors that limit the device performance. The current deposition techniques for CNT films still need to be improved in their compatibility with large-scale

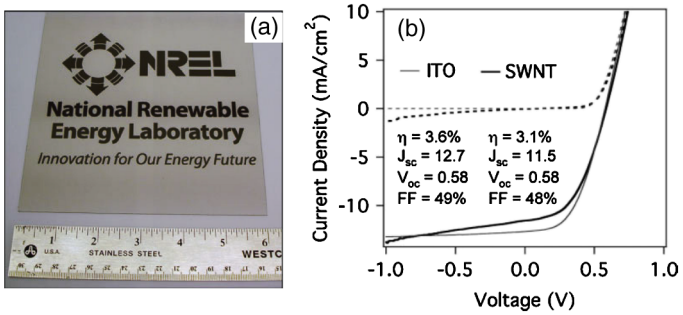

Fig. 8 (a) A photograph of single-walled carbon nanotube (SWNT) films (6×6 in.^{2}) by a spray deposition method. (b) J – V characteristics of P3HT:PCBM devices with ITO and SWNT transparent electrodes. Reprinted with permission from Ref. 189. Copyright 2009 John Wiley and Sons.

roll-to-roll processing. Moreover, there is very limited study of the mechanical flexibility and environmental stability of devices with CNT electrodes.

5.2 *Graphene*

Graphene is a two-dimensional material of close-packed carbon atoms with a honeycomb crystal lattice, which can be considered as a single atomic layer of graphite.[202] Since the great breakthrough from its theoretical study to experimental studies in 2004, which led to the Nobel Prize in physics in 2010,[203] graphene has attracted tremendous attention and presented many possible applications in different areas.[204,205] Similar to CNTs where all carbon atoms are connected with sp^2-bonds, a single graphene sheet exhibits high in-plane conductance since all valence electrons are delocalized over the entire sheet. Moreover, graphene shows excellent optical properties: a single graphene layer has a theoretical transmittance of 97.7% (with a reflectance of <0.1% and absorbance of ~2.3%).[34,206] Besides the excellent optical transparency and electrical conductivity, graphene also exhibits other impressive properties, such as great thermal and chemical stability, excellent mechanical properties (high flexibility and stretchability), and good interfacial contact with organic materials, which enables its potential application as TE in optoelectronic devices.[14,207–210]

Despite the promising properties of graphene as a TE, there are still several challenges remaining for its utilization in actual devices. Achieving high-quality graphene thin films and depositing graphene on required substrates is one of the biggest challenges. Since the pioneering report by Novoselov et al. in 2004,[211] mechanical exfoliation from bulk graphite materials is the basic technique to obtain high-quality graphene sheets for fundamental studies and small device demonstrations.[202,212,213] However, it is not suitable for high-throughput and large-scale industrial production lines. Chemical vapor deposition (CVD) is another successful technique for achieving graphene films,[32,47,214–216] which, despite its relatively high-cost deposition method with high treatment temperature, is still the most widely used fabrication method to obtain large graphene sheets. As shown in Figs. 9(a) and 9(b), Bae et al demonstrated large-scale (30-in.) CVD-grown graphene films with good flexibility and transparency. A monolayer of graphene film was first synthesized on copper foil using a CVD system, followed by some thermal and gas treatments for achieving high-quality films. A thermal-release tape was then attached with the graphene/copper foil for film transfer. After etching away the copper foil with copper etchant and cleaning the graphene surface with deionized water, the high-quality graphene film standing on the tape can be transferred to any target substrate.[215] Some solution-based deposition methods, such as liquid phase exfoliation and chemical reduction of graphene oxide, have also been developed to produce graphene films in the past several years. Direct exfoliation of graphite in specific solvents by sonication is the simple and low-cost method for graphene inks so far.[207,217] However, the concentration of graphene dispersed in these solvents, up to 1.5 mg/mL, is not high enough for some solution processes. Moreover, the mean flake size, generally on the order of 1 to 10 μm, is relatively small due to the sonication; therefore, films prepared from these solutions exhibit higher resistance as a result of significant junction resistances.[218] This approach can be further improved by adding volatile agents (e.g., alkali salt) and organic surfactants into the original graphite dispersions, where the ions or organic molecules can intercalate between graphite layers and expand the interlayer spacing, leading to improved exfoliation and a more stabilized and better-dispersed graphene solution with a higher concentration (up to 10 mg/mL).[219–221] Another alternative low-cost method is to reduce graphene oxide to graphene as demonstrated by several groups in the past few years, which provides a great opportunity to fabricate graphene inks or films on a large scale.[222–225] However, these solution methods, either exfoliation with metal ions and organic molecules or chemical reduction from oxides, induce a number of defects into the graphene sheets and interfaces, leading to a dramatic increase in the sheet resistance of the related graphene films.

Although a single graphene sheet exhibits a low sheet resistance of <100 $\Omega/\square$, most graphene films produced by the above methods show a high sheet resistance on the order of a 1 k$\Omega/\square$ range as a result of the possible structural defects and contact resistances between graphene flakes.[14,207,222] De Arco et al. reported high-quality graphene films synthesized by CVD with a sheet resistance of 230 $\Omega/\square$ and transmittance of 72% at $\lambda = 550$ nm. With such

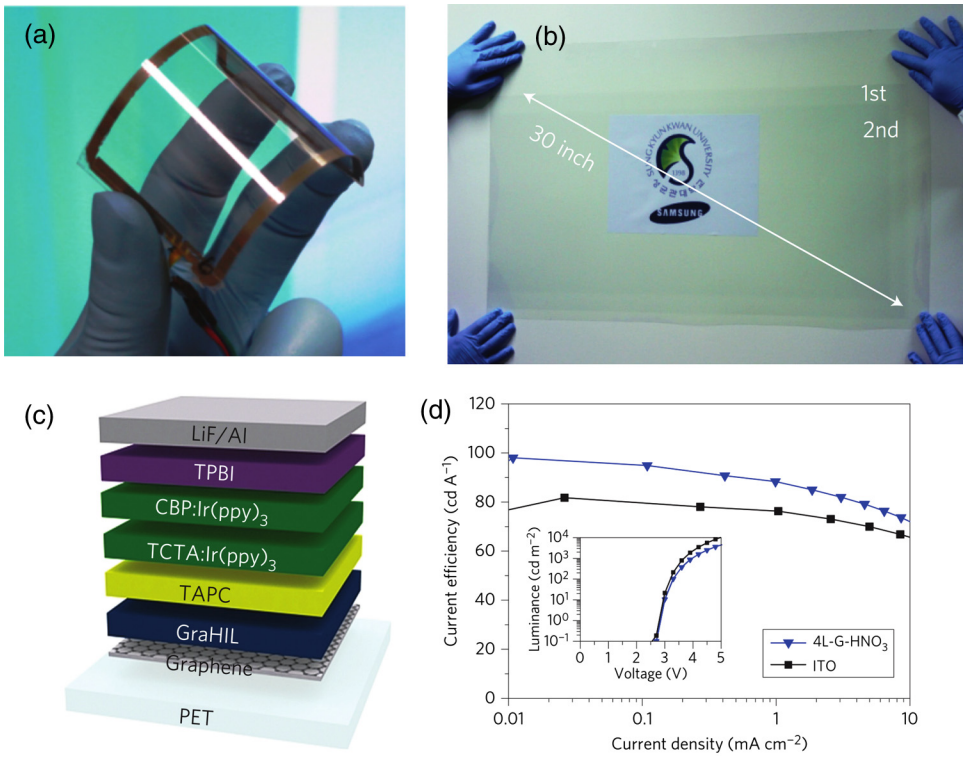

Fig. 9 (a) and (b) Photographs of flexible graphene layers grown by a chemical vapor deposition technique. Reprinted with permission from Ref. 215. Copyright 2010 Nature Publishing Group. (c) Device structure of flexible phosphorescent OLED with a graphene electrode. (d) Current efficiency and luminance (insert) of phosphorescent OLEDs with ITO and graphene as transparent electrodes. Reprinted with permission from Ref. 47. Copyright 2012 Nature Publishing Group.

graphene films as TEs, a small molecule CuPc/C_{60} PV device with an η_P of 1.18% was demonstrated, which was slightly lower than the ITO-reference cell ($\eta_P = 1.27\%$).[214] Some chemicals, such as $AuCl_4$,[31,32] HNO_3,[215] and thionyl chloride,[226] have shown doping effects to improve the conductivity of graphene layers while maintaining the high levels of transmittance. For example, a CVD-grown, four-layer graphene film doped with HNO_3 was demonstrated with a sheet resistance as low as 30 $\Omega/\square$ at ~90% transparency.[215] Han et al. used HNO_3 and $AuCl_4$ as p-dopants in CVD-grown graphene films and applied similar highly conductive graphene films to replace ITO in flexible OLEDs,[47] resulting in a decrease in sheet resistance from 87 to 54 and 34 $\Omega/\square$, respectively. These resistance values are now approaching that of ITO and thin metal layers, and are much higher than that of PEDOT:PSS and CNT layers. Using such highly conductive graphene to replace ITO in a green phosphorescent OLED [see Figs. 9(c) and 9(d)], a very high current efficiency phosphorescent OLED of up to 98.1 cd/A was achieved, which was appreciably higher than the ITO-reference cells (81.8 cd/A).[47]

Apart from improving the conductivity of graphene films, interfacial modification between graphene electrodes and active layers is another challenge in efficient optoelectronic devices. Similar to other possible TE candidates, polymers, such as PEDOT:PSS, and metal oxides, such as MoO_3, TiO_2, and ZnO, are widely utilized to modify graphene interface and minimize the possible energy barriers for efficient injection/extraction of electrons and holes. In some cases, some interfacial layers are required to improve the surface wettability for solution-processed transport/active layers. For instance, Zhang et al. introduced a layer of Al nanoclusters on a single-layer graphene to overcome its hydrophobic properties for TiO_2 deposition. As a result of such surface modification, the P3HT:PCBM devices with graphene as TE showed an η_P of ~2.6%, which was better than those without the modification and was close to that of the ITO-based references ($\eta_P = 3.45\%$).[227] These results suggest the great potential of using graphene as the TE in flexible organic optoelectronics. Moreover, graphene electrodes also possess outstanding mechanical flexibility.[14,216] De Arco et al. compared the graphene and ITO

conductance under different bending conditions: only minor changes in the film morphology and conductance were observed for graphene films after bending the films to 160 deg, whereas ITO films exhibited irreversible cracks and a decrease in conductance under 60 deg of bending.

Nevertheless, for large-area commercial applications, the resistance of the graphene layers needs to be further reduced, along with simplifying the graphene fabrication/transfer processes. Therefore, more effort is needed to obtain highly conductive graphene films with low-cost and large-scale deposition methods to enable its industrial application.

5.3 *Metal Nanowires*

Besides the carbon-based nanomaterials, films with random networks of metal NWs are also attractive candidates for transparent conductive electrodes.[18,228,229] Although many metal nanostructures, such as copper,[230,231] gold,[232,233] and cupronickel,[234] have been demonstrated with promising properties and possibility as electrodes, Ag NWs have been the focus of research in this area due to the excellent electrical properties of bulk Ag materials and the synthesis scalability of Ag NWs. Ag NWs with a typical diameter of 20 to 40 nm and length of $>20\ \mu$m dispersed in water or organic solvents are now commercially available.

Since metal NWs with proper surface treatment can be well dispersed in many solvents, many solution-based processing techniques, such as spin coating,[39] spray coating,[235,236] drop casting,[50] doctor blade coating,[11,237] Mayer rod coating,[40] brush painting,[238] etc., have been reported by different reach groups to achieve films with random NW networks. Similar to the discussion in CNTs, electrical and optical properties of the random NW networks are strongly dependent on the electrical properties of individual NWs, the interconnection between NWs, and the NW density in the resulting films. In general, the conductivity of NW networks increases as the length and diameter of an individual wire increases.[239] However, it is difficult to achieve NWs with an extremely long length and the typical reported length of Ag NWs is in the range of 1 to 50 μm. It is also challenging to maintain the integrity of very long NWs in the solid-state film, as they tend to break during the dispersion and deposition processes. Controlling the diameter of metal NWs is also critical for achieving high-quality films. NWs in thin films provide the conductive pathways for charge carrier transport, but they also function as scatter centers to incident light affecting the optical properties of the films. Therefore, the diameter of metal NWs should be minimized in order to achieve high optical transparency. Moreover, the diameter of individual NWs determines the surface roughness of films with random NW networks, which should also be reduced for most optoelectronic devices. Furthermore, an optimized wire density is required to balance between the electrical and optical properties for specific applications.

The junction resistance between the jointed wires is another dominant factor that affects the film resistance, which is similar to that for CNTs.[10,49] Several modification methods, such as thermal annealing,[35,228] optical sintering,[240] mechanical pressing,[241] and fusing with other materials,[42] have been demonstrated to reduce the junction resistance and improve the film conductivity. For example, Tokuno et al. applied a mechanical pressure of 25 MPa on as-deposited Ag NW films for 5 s at room temperature, which leads to a dramatic decrease in sheet resistance from $>10^4$ to 8.6 $\Omega/\square$.[241]

Several research groups have reported metal NW films with transmittance >85% and sheet resistance <20 $\Omega/\square$ [Figs. 10(a) and 10(b)], which are comparable with standard ITO electrodes, and explored them as TEs in organic optoelectronic devices.[11,39,242] Since the first application in small molecule OPVs that had an η_P only <0.5%, the overall performance of metal NW-based devices has been steadily advancing. Generally, a buffer layer (e.g., PEDOT:PSS, ZnO, or TiO_x) is required to flatten the surface of metal NW networks and to improve the contact with the active material so that they can serve as either anodes (collect/inject holes) or cathodes (collect/inject electrons) with proper buffer layers.[237,243–245] For instance, Leem et al. fabricated P3HT:PCBM cells with Ag NWs to replace the bottom ITO TE. With PEDOT:PSS and TiO_x as buffer layers, normal and inverted device architectures were achieved, respectively, which had comparable η_P of 2.0 and 3.5% compared to those of ITO-based reference cells.[39] Gaynor et al. successfully fabricated ITO-free white OLEDs with Ag NWs/poly (methyl methacrylate)

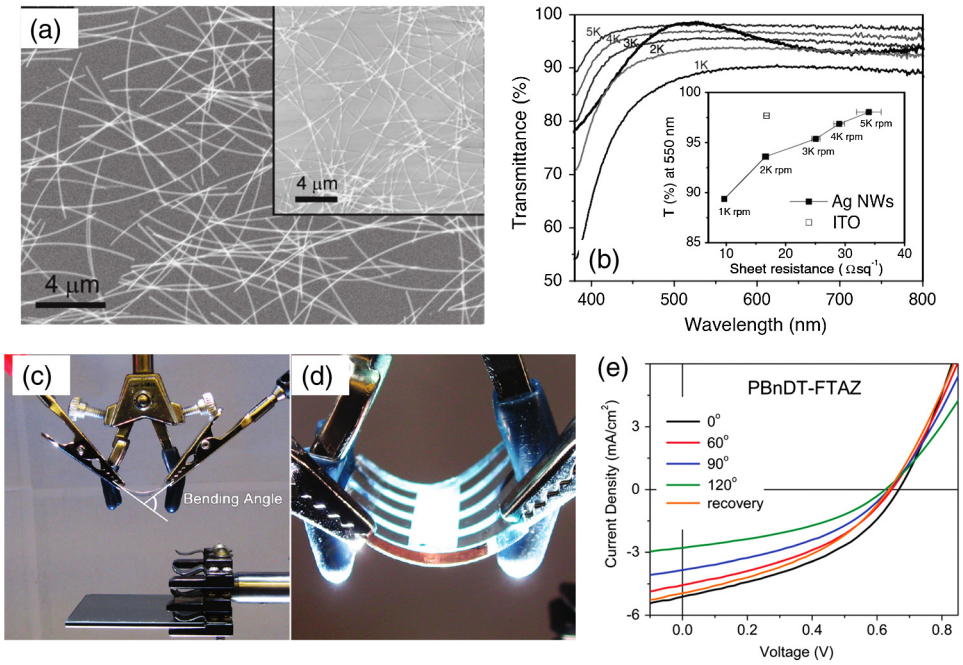

Fig. 10 (a) SEM image of a layer of Ag nanowires (NWs). (b) Transmittance and sheet resistance (insert) of Ag NW films with various thicknesses (different spin-speeds). Reprinted with permission from Ref. 39. Copyright 2011 John Wiley and Sons. (c) and (d) Experimental setup for measuring the flexibility of OPV devices with Ag NWs. (e) J – V characteristics of a flexible OPV device under different bending conditions. Reprinted with permission from Ref. 40. Copyright 2011 American Chemical Society.

composites as TEs, which showed a luminous efficiency >30 lm/W and were close to that of the ITO-based devices (35.8 lm/W).[246] The solution-processibility of metal NWs also offers a great opportunity to make them as transparent top electrodes for organic optoelectronic devices. For example, Chen et al. successfully applied Ag NW electrodes in a high-performance polymer solar cell to achieve a visibly transparent device, where the ITO and ITO-nanoparticles-fused Ag NW layers serve as the bottom and top TEs, respectively. Such transparent devices showed efficiencies of $\eta_P = 4.0$ and 3.8% when illuminated from ITO and Ag NW electrodes, respectively, and a maximum transmittance of ~60% in the visible light range.[247] Great mechanical properties are also the advantages of metal NW networks compared to ITO substrates.[40,88,248,249] As shown in Figs. 10(c) to 10(e), Yang et al. demonstrated the flexibility of Ag NW electrode based OPV devices on flexible substrates, which exhibited a recoverable efficiency under a bending angle of 120 deg.[40] Akter and Kim also studied the stretchability of Ag NW films, where the conductivity of the electrode remained unchanged with ~20% elongation.[248]

The above great device performance and excellent mechanical stability suggest the strong potential of using random metal NW networks as transparent conductive electrodes. However, several challenges still remain to be solved. For instance, the poor adhesion between the metal NWs and substrates limits their compatibility with different substrates. Adding some adhesive layers at the NW/substrate interface or treating metal NW surface with proper ligands to make them better anchored on substrates are some possible approaches to promote the adhesion.[228] The long-term stability of metal NW electrodes is another concern for their application in electronic devices. There has been some evidence suggesting that electromigration of metal atoms along the NWs causes failure of the wires and the entire network. This is especially important for devices that require high operation current, in which case the film conductivity keeps decreasing until their full breakdown.[250,251] Moreover, some metal NWs (e.g., Ag NWs) can be corroded through chemical reactions, such as oxidation and suffixation, which also cause the degradation of metal NWs and their related devices.

6 Conclusion

To date, ITO has been the most widely used material as transparent conductive electrodes in organic optoelectronic devices (OPVs and OLEDs). However, the rising cost of ITO, as a result of the scarcity of indium along with the increased demands, competes with the low-cost nature of organic-based devices. Therefore, searching for ITO alternatives becomes critical for the commercialization of low-cost OPVs and OLEDs. Various emerging materials have been reported as transparent conductive electrodes in optoelectronic devices, though not all of them show better properties than ITO. Thin metals are one of the alternatives to ITO, where their excellent ductility makes them suitable for flexible applications. However, the relatively low transparency of ultrathin metal layers limits the performance of their related devices. Conductive transparent polymers have emerged as low-cost electrodes over the last 10 years due to the great solution compatibility and large-scale processibility, but suffer from poor electrical properties and environmental stability. Nanomaterials, such as CNTs, graphenes, and metal NWs, have emerged as other attractive candidates as ITO alternatives. CNTs and graphenes have been studied extensively; however, they are still a long way from commercial applications as transparent conductive electrodes because of their low film conductivities and limited large-scale process techniques. Metal NWs, with their promising optoelectronic properties and good compatibility with most solution-based processes, are another top-rated material as transparent conductors, though several issues remain to be solved. The high surface roughness and poor electrical and environmental stability impede their applications in devices with ultrathin layers.

Other than the focusing on one single material, the combination of two or more different materials, such as metal grid/polymer, metal NWs/polymer, graphene/metal grids, thin metal/graphene, etc., shows improved performance as transparent electrodes by complementing the good properties of each material.[252,253] This also open up more routes for searching TEs in optoelectronic devices. Overall, with cheap raw materials and good compatibility with environment-friendly deposition processes, we believe that these attractive materials will be adapted for application as TEs in optoelectronic devices.

Acknowledgments

The authors gratefully acknowledge partial financial support from the Research Corporation for Science Advancement and the University of Florida Office of Research.

References

1. S. R. Forrest, "The path to ubiquitous and low-cost organic electronic appliances on plastic," *Nature* **428**(6986), 911–918 (2004).
2. J. Xue, "Perspectives on organic photovoltaics," *Polym. Rev.* **50**(4), 411–419 (2010).
3. N. Espinosa et al., "Solar cells with one-day energy payback for the factories of the future," *Energy Environ. Sci.* **5**(1), 5117–5132 (2012).
4. W. Cao and J. Xue, "Recent progress in organic photovoltaics: device architecture and optical design," *Energy Environ. Sci.* **7**, 2123–2144 (2014).
5. G. Li, R. Zhu, and Y. Yang, "Polymer solar cells," *Nat. Photonics* **6**(3), 153–161 (2012).
6. M. A. Green et al., "Solar cell efficiency tables (version 43)," *Prog. Photovoltaics* **22**(1), 1–9 (2014).
7. C. W. Tang, "2-layer organic photovoltaic cell," *Appl. Phys. Lett.* **48**(2), 183–185 (1986).
8. C. W. Tang and S. A. Vanslyke, "Organic electroluminescent diodes," *Appl. Phys. Lett.* **51**(12), 913–915 (1987).
9. J. Xue and S. R. Forrest, "Carrier transport in multilayer organic photodetectors. II. Effects of anode preparation," *J. Appl. Phys.* **95**(4), 1869–1877 (2004).
10. D. S. Hecht, L. Hu, and G. Irvin, "Emerging transparent electrodes based on thin films of carbon nanotubes, graphene, and metallic nanostructures," *Adv. Mater.* **23**(13), 1482–1513 (2011).
11. J. Krantz et al., "Solution-processed metallic nanowire electrodes as indium tin oxide replacement for thin-film solar cells," *Adv. Funct. Mater.* **21**(24), 4784–4787 (2011).

12. A. Sandstrom et al., "Ambient fabrication of flexible and large-area organic light-emitting devices using slot-die coating," *Nat. Commun.* **3**, 1002 (2012).
13. S.-I. Na et al., "Efficient and flexible ITO-free organic solar cells using highly conductive polymer anodes," *Adv. Mater.* **20**(21), 4061–4067 (2008).
14. K. S. Kim et al., "Large-scale pattern growth of graphene films for stretchable transparent electrodes," *Nature* **457**(7230), 706–710 (2009).
15. D. Gupta, M. M. Wienk, and R. A. J. Janssen, "Efficient polymer solar cells on opaque substrates with a laminated PEDOT:PSS top electrode," *Adv. Energy Mater.* **3**(6), 782–787 (2013).
16. A. Kumar and C. Zhou, "The race to replace tin-doped indium oxide: which material will win?," *ACS Nano* **4**(1), 11–14 (2010).
17. F. Zhang et al., "Polymer photovoltaic cells with conducting polymer anodes," *Adv. Mater.* **14**(9), 662–665 (2002).
18. W. Gaynor, J.-Y. Lee, and P. Peumans, "Fully solution-processed inverted polymer solar cells with laminated nanowire electrodes," *ACS Nano* **4**(1), 30–34 (2010).
19. A. D. Pasquier et al., "Conducting and transparent single-wall carbon nanotube electrodes for polymer-fullerene solar cells," *Appl. Phys. Lett.* **87**(20), 203511 (2005).
20. M. W. Rowell et al., "Organic solar cells with carbon nanotube network electrodes," *Appl. Phys. Lett.* **88**(23), 233506 (2006).
21. V. Bhosle et al., "Gallium-doped zinc oxide films as transparent electrodes for organic solar cell applications," *J. Appl. Phys.* **102**(2), 023501 (2007).
22. J. Y. Lee et al., "Solution-processed metal nanowire mesh transparent electrodes," *Nano Lett.* **8**(2), 689–692 (2008).
23. M.-G. Kang et al., "Organic solar cells using nanoimprinted transparent metal electrodes," *Adv. Mater.* **20**(23), 4408–4413 (2008).
24. T. Minami, "Substitution of transparent conducting oxide thin films for indium tin oxide transparent electrode applications," *Thin Solid Films* **516**(7), 1314–1321 (2008).
25. A. M. Nardes et al., "Conductivity, work function, and environmental stability of PEDOT:PSS thin films treated with sorbitol," *Org. Electron.* **9**(5), 727–734 (2008).
26. Y. Feng et al., "Organic solar cells using few-walled carbon nanotubes electrode controlled by the balance between sheet resistance and the transparency," *Appl. Phys. Lett.* **94**(12), 123302 (2009).
27. E. Vitoratos et al., "Thermal degradation mechanisms of PEDOT:PSS," *Org. Electron.* **10**(1), 61–66 (2009).
28. M. Choe et al., "Efficient bulk-heterojunction photovoltaic cells with transparent multi-layer graphene electrodes," *Org. Electron.* **11**(11), 1864–1869 (2010).
29. S. De et al., "Size effects and the problem with percolation in nanostructured transparent conductors," *ACS Nano* **4**(12), 7064–7072 (2010).
30. S. Kim et al., "Spin- and spray-deposited single-walled carbon-nanotube electrodes for organic solar cells," *Adv. Funct. Mater.* **20**(14), 2310–2316 (2010).
31. K. K. Kim et al., "Enhancing the conductivity of transparent graphene films via doping," *Nanotechnology* **21**(28), 285205 (2010).
32. H. Park et al., "Doped graphene electrodes for organic solar cells," *Nanotechnology* **21**(50), 505204 (2010).
33. H. Saarenpaa et al., "Aluminum doped zinc oxide films grown by atomic layer deposition for organic photovoltaic devices," *Sol. Energy Mater. Sol. Cells* **94**(8), 1379–1383 (2010).
34. J. Wu et al., "Organic light-emitting diodes on solution-processed graphene transparent electrodes," *ACS Nano* **4**(1), 43–48 (2010).
35. X.-Y. Zeng et al., "A new transparent conductor: silver nanowire film buried at the surface of a transparent polymer," *Adv. Mater.* **22**(40), 4484–4488 (2010).
36. C.-K. Cho et al., "Mechanical flexibility of transparent PEDOT:PSS electrodes prepared by gravure printing for flexible organic solar cells," *Sol. Energy Mater. Sol. Cells* **95**(12), 3269–3275 (2011).
37. Y. H. Kim et al., "Highly conductive PEDOT:PSS electrode with optimized solvent and thermal post-treatment for ITO-free organic solar cells," *Adv. Funct. Mater.* **21**(6), 1076–1081 (2011).

38. D. S. Hecht and R. B. Kaner, "Solution-processed transparent electrodes," *MRS Bull.* **36**(10), 749–755 (2011).
39. D. S. Leem et al., "Efficient organic solar cells with solution-processed silver nanowire electrodes," *Adv. Mater.* **23**(38), 4371–4375 (2011).
40. L. Yang et al., "Solution-processed flexible polymer solar cells with silver nanowire electrodes," *ACS Appl. Mater. Interfaces* **3**(10), 4075–4084 (2011).
41. S. D. Yambem et al., "Optimization of organic solar cells with thin film Au as anode," *Sol. Energy Mater. Sol. Cells* **95**(8), 2424–2430 (2011).
42. R. Zhu et al., "Fused silver nanowires with metal oxide nanoparticles and organic polymers for highly transparent conductors," *ACS Nano* **5**(12), 9877–9882 (2011).
43. T. M. Barnes et al., "Comparing the fundamental physics and device performance of transparent, conductive nanostructured networks with conventional transparent conducting oxides," *Adv. Energy Mater.* **2**(3), 353–360 (2012).
44. W. Cao et al., "Flexible organic solar cells using an oxide/metal/oxide trilayer as transparent electrode," *Org. Electron.* **13**(11), 2221–2228 (2012).
45. K. Ellmer, "Past achievements and future challenges in the development of optically transparent electrodes," *Nat. Photonics* **6**(12), 808–816 (2012).
46. N. Formica et al., "Highly stable Ag-Ni based transparent electrodes on PET substrates for flexible organic solar cells," *Sol. Energy Mater. Sol. Cells* **107**, 63–68 (2012).
47. T.-H. Han et al., "Extremely efficient flexible organic light-emitting diodes with modified graphene anode," *Nat. Photonics* **6**(2), 105–110 (2012).
48. M. Vosgueritchian, D. J. Lipomi, and Z. Bao, "Highly conductive and transparent PEDOT:PSS films with a fluorosurfactant for stretchable and flexible transparent electrodes," *Adv. Funct. Mater.* **22**(2), 421–428 (2012).
49. D. Langley et al., "Flexible transparent conductive materials based on silver nanowire networks: a review," *Nanotechnology* **24**(45), 452001 (2013).
50. M. Reinhard et al., "Solution-processed polymer-silver nanowire top electrodes for inverted semi-transparent solar cells," *Org. Electron.* **14**(1), 273–277 (2013).
51. W. Zhang et al., "High-efficiency ITO-free polymer solar cells using highly conductive PEDOT:PSS/surfactant bilayer transparent anodes," *Energy Environ. Sci.* **6**(6), 1956–1964 (2013).
52. J.-S. Yu et al., "Transparent conductive film with printable embedded patterns for organic solar cells," *Sol. Energy Mater. Sol. Cells* **109**, 142–147 (2013).
53. D. Y. Cho et al., "Highly flexible and stretchable carbon nanotube network electrodes prepared by simple brush painting for cost-effective flexible organic solar cells," *Carbon* **66**, 530–538 (2014).
54. T. Minami, "Transparent conducting oxide semiconductors for transparent electrodes," *Semicond. Sci. Techol.* **20**(4), S35–S44 (2005).
55. I. Irfan et al., "Interplay of cleaning and de-doping in oxygen plasma treated high work function indium tin oxide (ITO)," *Org. Electron.* **13**(10), 2028–2034 (2012).
56. D. J. Milliron et al., "Surface oxidation activates indium tin oxide for hole injection," *J. Appl. Phys.* **87**(1), 572–576 (2000).
57. C. N. Li et al., "Improved performance of OLEDs with ITO surface treatments," *Thin Solid Films* **477**(1–2), 57–62 (2005).
58. Y. Park et al., "Work function of indium tin oxide transparent conductor measured by photoelectron spectroscopy," *Appl. Phys. Lett.* **68**(19), 2699–2701 (1996).
59. K. Sugiyama et al., "Dependence of indium-tin-oxide work function on surface cleaning method as studied by ultraviolet and x-ray photoemission spectroscopies," *J. Appl. Phys.* **87**(1), 295–298 (2000).
60. K. Sun and J. Ouyang, "Polymer solar cells using chlorinated indium tin oxide electrodes with high work function as the anode," *Sol. Energy Mater. Sol. Cells* **96**(1), 238–243 (2012).
61. Z. R. Hong et al., "Characterization of organic photovoltaic devices with indium-tin-oxide anode treated by plasma in various gases," *J. Appl. Phys.* **100**(9), 093711 (2006).
62. P. Destruel et al., "Influence of indium tin oxide treatment using UV-ozone and argon plasma on the photovoltaic parameters of devices based on organic discotic materials," *Polym. Int.* **55**(6), 601–607 (2006).

63. J. H. Huang et al., "Electrochemical characterization of the solvent-enhanced conductivity of poly(3,4-ethylenedioxythiophene) and its application in polymer solar cells," *J. Mater. Chem.* **19**(22), 3704–3712 (2009).
64. B. Peng et al., "Performance improvement of polymer solar cells by using a solvent-treated poly(3,4-ethylenedioxythiophene):poly(styrenesulfonate) buffer layer," *Appl. Phys. Lett.* **98**(24), 243308 (2011).
65. M. D. Irwin et al., "Structural and electrical functionality of NiO interfacial films in bulk heterojunction organic solar cells," *Chem. Mater.* **23**(8), 2218–2226 (2011).
66. S. R. Hammond et al., "Low-temperature, solution-processed molybdenum oxide hole-collection layer for organic photovoltaics," *J. Mater. Chem.* **22**(7), 3249–3254 (2012).
67. J. Meyer et al., "Transition metal oxides for organic electronics: energetics, device physics and applications," *Adv. Mater.* **24**(40), 5408–5427 (2012).
68. J. R. Manders et al., "Solution-processed nickel oxide hole transport layers in high efficiency polymer photovoltaic cells," *Adv. Funct. Mater.* **23**(23), 2993–3001 (2013).
69. C. Waldauf et al., "Highly efficient inverted organic photovoltaics using solution based titanium oxide as electron selective contact," *Appl. Phys. Lett.* **89**(23), 233517 (2006).
70. S. K. Hau et al., "Air-stable inverted flexible polymer solar cells using zinc oxide nanoparticles as an electron selective layer," *Appl. Phys. Lett.* **92**(25), 253301 (2008).
71. L. Qian et al., "Hybrid polymer-CdSe solar cells with a ZnO nanoparticle buffer layer for improved efficiency and lifetime," *J. Mater. Chem.* **21**(11), 3814–3817 (2011).
72. Y. M. Sun et al., "Inverted polymer solar cells integrated with a low-temperature-annealed sol-gel-derived ZnO film as an electron transport layer," *Adv. Mater.* **23**(14), 1679–1683 (2011).
73. R. Zhou et al., "Solution-processed, nanostructured hybrid solar cells with broad spectral sensitivity and stability," *Nanoscale* **4**(11), 3507–3514 (2012).
74. P. K. H. Ho et al., "Molecular-scale interface engineering for polymer light-emitting diodes," *Nature* **404**(6777), 481–484 (2000).
75. H. Yan et al., "High-brightness blue light-emitting polymer diodes via anode modification using a self-assembled monolayer," *Adv. Mater.* **15**(10), 835–838 (2003).
76. S. Khodabakhsh et al., "Using self-assembling dipole molecules to improve hole injection in conjugated polymers," *Adv. Funct. Mater.* **14**(12), 1205–1210 (2004).
77. J. S. Kim et al., "Control of the electrode work function and active layer morphology via surface modification of indium tin oxide for high efficiency organic photovoltaics," *Appl. Phys. Lett.* **91**(11), 112111 (2007).
78. M. G. Helander et al., "Chlorinated indium tin oxide electrodes with high work function for organic device compatibility," *Science* **332**(6032), 944–947 (2011).
79. T. Dobbertin et al., "Inverted top-emitting organic light-emitting diodes using sputter-deposited anodes," *Appl. Phys. Lett.* **82**(2), 284–286 (2003).
80. H.-K. Kim et al., "Plasma damage-free sputtering of indium tin oxide cathode layers for top-emitting organic light-emitting diodes," *Appl. Phys. Lett.* **86**(18), 183503 (2005).
81. G. Parthasarathy et al., "A metal-free cathode for organic semiconductor devices," *Appl. Phys. Lett.* **72**(17), 2138–2140 (1998).
82. P. E. Burrows et al., "Semitransparent cathodes for organic light emitting devices," *J. Appl. Phys.* **87**(6), 3080–3085 (2000).
83. H. Schmidt et al., "Efficient semitransparent inverted organic solar cells with indium tin oxide top electrode," *Appl. Phys. Lett.* **94**(24), 243302 (2009).
84. G. Gu et al., "Transparent stacked organic light emitting devices. I. Design principles and transparent compound electrodes," *J. Appl. Phys.* **86**(8), 4067–4075 (1999).
85. D. Kim et al., "Low temperature deposition of ITO thin films by ion beam sputtering," *Thin Solid Films* **377**, 81–86 (2000).
86. Y. Hoshi and T. Kiyomura, "ITO thin films deposited at low temperatures using a kinetic energy controlled sputter-deposition technique," *Thin Solid Films* **411**(1), 36–41 (2002).
87. P. E. Burrows et al., "Semitransparent cathodes for organic light emitting devices," *J. Appl. Phys.* **87**(6), 3080–3085 (2000).
88. M. Song et al., "Highly efficient and bendable organic solar cells with solution-processed silver nanowire electrodes," *Adv. Funct. Mater.* **23**(34), 4177–4184 (2013).

89. E. Fortunato et al., "Transparent conducting oxides for photovoltaics," *MRS Bull.* **32**(3), 242–247 (2007).
90. J. Meyer et al., "Indium-free transparent organic light emitting diodes with Al doped ZnO electrodes grown by atomic layer and pulsed laser deposition," *Appl. Phys. Lett.* **93**(7), 073308 (2008).
91. H. Liu et al., "Efficient and ultraviolet durable inverted organic solar cells based on an aluminum-doped zinc oxide transparent cathode," *Appl. Phys. Lett.* **103**(4), 043309 (2013).
92. J.-H. Park et al., "Effects of deposition temperature on characteristics of Ga-doped ZnO film prepared by highly efficient cylindrical rotating magnetron sputtering for organic solar cells," *Sol. Energy Mater. Sol. Cells* **95**(2), 657–663 (2011).
93. X. Jiang et al., "Aluminum-doped zinc oxide films as transparent conductive electrode for organic light-emitting devices," *Appl. Phys. Lett.* **83**(9), 1875–1877 (2003).
94. W. Wang et al., "Dependence of aluminum-doped zinc oxide work function on surface cleaning method as studied by ultraviolet and x-ray photoelectron spectroscopies," *Appl. Surf. Sci.* **257**(9), 3884–3887 (2011).
95. Z. Hu et al., "Highly efficient organic photovoltaic devices using F-doped SnO2 anodes," *Appl. Phys. Lett.* **98**(12), 123302 (2011).
96. M. Liu, M. B. Johnston, and H. J. Snaith, "Efficient planar heterojunction perovskite solar cells by vapour deposition," *Nature* **501**(7467), 395–398 (2013).
97. M. M. Lee et al., "Efficient hybrid solar cells based on meso-superstructured organometal halide perovskites," *Science* **338**(6107), 643–647 (2012).
98. J. Burschka et al., "Sequential deposition as a route to high-performance perovskite-sensitized solar cells," *Nature* **499**(7458), 316 (2013).
99. S. H. Park, J. B. Park, and P. K. Song, "Characteristics of Al-doped, Ga-doped and In-doped zinc-oxide films as transparent conducting electrodes in organic light-emitting diodes," *Curr. Appl. Phys.* **10**(3), S488–S490 (2010).
100. R. B. Pode et al., "Transparent conducting metal electrode for top emission organic light-emitting devices: Ca-Ag double layer," *Appl. Phys. Lett.* **84**(23), 4614–4616 (2004).
101. M. Al-Ibrahim et al., "Comparison of normal and inverse poly(3-hexylthiophene)/fullerene solar cell architectures," *Sol. Energy Mater. Sol. Cells* **85**(2), 277–283 (2005).
102. R. F. Bailey-Salzman, B. P. Rand, and S. R. Forrest, "Semitransparent organic photovoltaic cells," *Appl. Phys. Lett.* **88**(23), 233502 (2006).
103. B. O'Connor et al., "Transparent and conductive electrodes based on unpatterned, thin metal films," *Appl. Phys. Lett.* **93**(22), 223304 (2008).
104. S. Wilken et al., "ITO-free inverted polymer/fullerene solar cells: interface effects and comparison of different semi-transparent front contacts," *Sol. Energy Mater. Sol. Cells* **96**(1), 141–147 (2012).
105. K.-S. Chen et al., "Semi-transparent polymer solar cells with 6% PCE, 25% average visible transmittance and a color rendering index close to 100 for power generating window applications," *Energy Environ. Sci.* **5**(11), 9551–9557 (2012).
106. S. D. Yambem, K. Liao, and S. A. Curran, "Flexible Ag electrode for use in organic photovoltaics," *Sol. Energy Mater. Sol. Cells* **95**(11), 3060–3064 (2011).
107. S. Cheylan et al., "Organic light-emitting diode with indium-free metallic bilayer as transparent anode," *Org. Electron.* **12**(5), 818–822 (2011).
108. E. H.-E. Wu et al., "Controlling optical properties of electrodes with stacked metallic thin films for polymeric light-emitting diodes and displays," *J. Disp. Technol.* **1**(1), 105–111 (2005).
109. H. M. Stec et al., "Ultrathin transparent Au electrodes for organic photovoltaics fabricated using a mixed mono-molecular nucleation layer," *Adv. Funct. Mater.* **21**(9), 1709–1716 (2011).
110. S. Schubert et al., "Improvement of transparent metal top electrodes for organic solar cells by introducing a high surface energy seed layer," *Adv. Energy Mater.* **3**(4), 438–443 (2013).
111. C. J. Lee et al., "Red electrophosphorescent top emission organic light-emitting device with Ca/Ag semitransparent cathode," *Appl. Phys. Lett.* **89**(25), 253508 (2006).

112. A. Haldar et al., "Organic photovoltaics using thin gold film as an alternative anode to indium tin oxide," *Thin Solid Films* **519**(18), 6169–6173 (2011).
113. J. C. C. Fan et al., "Transparent heat-mirror films of Tio_2/Ag/Tio_2 for solar-energy collection and radiation insulation," *Appl. Phys. Lett.* **25**(12), 693–695 (1974).
114. W. Ji et al., "High-color-rendering flexible top-emitting warm-white organic light emitting diode with a transparent multilayer cathode," *Org. Electron.* **12**(7), 1137–1141 (2011).
115. H. Jin et al., "Efficient, large area ITO-and-PEDOT-free organic solar cell sub-modules," *Adv. Mater.* **24**(19), 2572–2577 (2012).
116. E. Wrzesniewski et al., "Enhancing light extraction in top-emitting organic light-emitting devices using molded transparent polymer microlens arrays," *Small* **8**(17), 2647–2651 (2012).
117. M. Kohlstadt et al., "Inverted ITO- and PEDOT:PSS-free polymer solar cells with high power conversion efficiency," *Sol. Energy Mater. Sol. Cells* **117**, 98–102 (2013).
118. N. P. Sergeant et al., "Design of transparent anodes for resonant cavity enhanced light harvesting in organic solar cells," *Adv. Mater.* **24**(6), 728–732 (2012).
119. K.-H. Choi et al., "Highly flexible and transparent InZnSnOx/Ag/InZnSnOx multilayer electrode for flexible organic light emitting diodes," *Appl. Phys. Lett.* **92**(22), 223302 (2008).
120. E. Wrzesniewski et al., "Transparent oxide/metal/oxide trilayer electrode for use in top-emitting organic light-emitting diodes," *J. Photon. Energy* **1**, 011023 (2011).
121. L. Cattin et al., "Investigation of low resistance transparent MoO3/Ag/MoO3 multilayer and application as anode in organic solar cells," *Thin Solid Films* **518**(16), 4560–4563 (2010).
122. S.-H. Choa et al., "Mechanical integrity of flexible InZnO/Ag/InZnO multilayer electrodes grown by continuous roll-to-roll sputtering," *Sol. Energy Mater. Sol. Cells* **95**(12), 3442–3449 (2011).
123. H. Cho et al., "Highly flexible organic light-emitting diodes based on ZnS/Ag/WO3 multilayer transparent electrodes," *Org. Electron.* **10**(6), 1163–1169 (2009).
124. K. Hong et al., "Optical properties of WO3/Ag/WO3 multi layer as transparent cathode in top-emitting organic light emitting diodes," *J. Phys. Chem. C* **115**(8), 3453–3459 (2011).
125. H. Cho, C. Yun, and S. Yoo, "Multilayer transparent electrode for organic light-emitting diodes: tuning its optical characteristics," *Opt. Express* **18**(4), 3404–3414 (2010).
126. Y. C. Han et al., "ITO-free flexible organic light-emitting diode using ZnS/Ag/MoO3 anode incorporating a quasi-perfect Ag thin film," *Org. Electron.* **14**(12), 3437–3443 (2013).
127. G. H. Jung et al., "BCP/Ag/MoO3 transparent cathodes for organic photovoltaics," *Adv. Energy Mater.* **1**(6), 1023–1028 (2011).
128. S. Lim et al., "Cu-based multilayer transparent electrodes: a low-cost alternative to ITO electrodes in organic solar cells," *Sol. Energy Mater. Sol. Cells* **101**, 170–175 (2012).
129. B. Tian et al., "Transparent organic light-emitting devices using a MoO3/Ag/MoO3 cathode," *J. Appl. Phys.* **110**(10), 104507 (2011).
130. J.-A. Jeong and H.-K. Kim, "Low resistance and highly transparent ITO-Ag-ITO multilayer electrode using surface plasmon resonance of Ag layer for bulk-heterojunction organic solar cells," *Sol. Energy Mater. Sol. Cells* **93**(10), 1801–1809 (2009).
131. F. Roca et al., "Process development of amorphous silicon crystalline silicon solar cells," *Sol. Energy Mater. Sol. Cells* **48**(1–4), 15–24 (1997).
132. U. P. Singh and S. P. Patra, "Progress in polycrystalline thin-film Cu(In,Ga)Se-2 solar cells," *Int. J. Photoenergy* **2010**, 468147 (2010).
133. M.-G. Kang et al., "Transparent Cu nanowire mesh electrode on flexible substrates fabricated by transfer printing and its application in organic solar cells," *Sol. Energy Mater. Sol. Cells* **94**(6), 1179–1184 (2010).
134. C. Min et al., "Enhancement of optical absorption in thin-film organic solar cells through the excitation of plasmonic modes in metallic gratings," *Appl. Phys. Lett.* **96**(13), 133302 (2010).
135. Y. Galagan et al., "ITO-free flexible organic solar cells with printed current collecting grids," *Sol. Energy Mater. Sol. Cells* **95**(5), 1339–1343 (2011).

136. J. Zou et al., "Metal grid/conducting polymer hybrid transparent electrode for inverted polymer solar cells," *Appl. Phys. Lett.* **96**(20), 203301 (2010).
137. M.-G. Kang et al., "Efficiency enhancement of organic solar cells using transparent plasmonic Ag nanowire electrodes," *Adv. Mater.* **22**(39), 4378–4383 (2010).
138. Y.-H. Ho et al., "Transparent and conductive metallic electrodes fabricated by using nanosphere lithography," *Org. Electron.* **12**(6), 961–965 (2011).
139. M.-G. Kang and L. J. Guo, "Nanoimprinted semitransparent metal electrodes and their application in organic light-emitting diodes," *Adv. Mater.* **19**(10), 1391–1396 (2007).
140. M.-G. Kang and L. J. Guo, "Semitransparent Cu electrode on a flexible substrate and its application in organic light emitting diodes," *J. Vac. Sci. Technol. B* **25**(6), 2637–2641 (2007).
141. K. Tvingstedt and O. Inganas, "Electrode grids for ITO-free organic photovoltaic devices," *Adv. Mater.* **19**(19), 2893–2897 (2007).
142. T. W. Lee et al., "Soft-contact optical lithography using transparent elastomeric stamps: application to nanopatterned organic light-emitting devices," *Adv. Funct. Mater.* **15**(9), 1435–1439 (2005).
143. S. K. Hau et al., "Indium tin oxide-free semi-transparent inverted polymer solar cells using conducting polymer as both bottom and top electrodes," *Org. Electron.* **10**(7), 1401–1407 (2009).
144. Y. Zhou et al., "Indium tin oxide-free and metal-free semitransparent organic solar cells," *Appl. Phys. Lett.* **97**(15), 153304 (2010).
145. Y.-S. Hsiao et al., "All-solution-processed inverted polymer solar cells on granular surface-nickelized polyimide," *Org. Electron.* **10**(4), 551–561 (2009).
146. R. Po et al., "The role of buffer layers in polymer solar cells," *Energy Environ. Sci.* **4**(2), 285–310 (2011).
147. F. Nickel et al., "Cathodes comprising highly conductive poly(3,4-ethylenedioxythiophene): poly(styrenesulfonate) for semi-transparent polymer solar cells," *Org. Electron.* **11**(4), 535–538 (2010).
148. Y. Zhou et al., "Optimization of a polymer top electrode for inverted semitransparent organic solar cells," *Org. Electron.* **12**(5), 827–831 (2011).
149. B. Ouyang et al., "High-conductivity poly (3,4-ethylenedioxythiophene): poly(styrene sulfonate) film and its application in polymer optoelectronic devices," *Adv. Funct. Mater.* **15**(2), 203–208 (2005).
150. J.-R. Kim et al., "Efficient TCO-free organic solar cells with modified poly(3,4-ethylenedioxythiophene): poly(styrenesulfonate) anodes," *J. Nanosci. Nanotechnol.* **11**(1), 326–330 (2011).
151. Y.-S. Hsiao et al., "High-conductivity poly(3,4-ethylenedioxythiophene):poly(styrene sulfonate) film for use in ITO-free polymer solar cells," *J. Mater. Chem.* **18**(48), 5948–5955 (2008).
152. S. Admassie et al., "A polymer photodiode using vapour-phase polymerized PEDOT as an anode," *Sol. Energy Mater. Sol. Cells* **90**(2), 133–141 (2006).
153. P. A. Levermore et al., "High efficiency organic light-emitting diodes with PEDOT-based conducting polymer anodes," *J. Mater. Chem.* **18**(37), 4414–4420 (2008).
154. G. Wang, X. Tao, and R. Wang, "Flexible organic light-emitting diodes with a polymeric nanocomposite anode," *Nanotechnology* **19**(14), 145201 (2008).
155. Y. Wang et al., "An efficient flexible white organic light-emitting device with a screen-printed conducting polymer anode," *J. Phys. D Appl. Phys.* **45**(40), 402002 (2012).
156. D. A. Mengistie et al., "Highly conductive PEDOT:PSS treated with formic acid for ITO-free polymer solar cells," *ACS Appl. Mater. Interfaces* **6**(4), 2290–2297 (2014).
157. T.-S. Kim et al., "All-solution-processed ITO-free polymer solar cells fabricated on copper sheets," *Sol. Energy Mater. Sol. Cells* **98**, 168–171 (2012).
158. D. J. Lipomi et al., "Electronic properties of transparent conductive films of PEDOT:PSS on stretchable substrates," *Chem. Mater.* **24**(2), 373–382 (2012).
159. Y.-C. Huang et al., "High-performance ITO-free spray-processed polymer solar cells with incorporating ink-jet printed grid," *Org. Electron.* **14**(11), 2809–2817 (2013).

160. H. J. Lee et al., "Negative mold transfer patterned conductive polymer electrode for flexible organic light-emitting diodes," *Org. Electron.* **14**(1), 416–422 (2013).
161. Q. Dong et al., "All-spin-coating vacuum-free processed semi-transparent inverted polymer solar cells with PEDOT:PSS anode and PAH-D interfacial layer," *Org. Electron.* **11**(7), 1327–1331 (2010).
162. S. K. Hau et al., "Interfacial modification to improve inverted polymer solar cells," *J. Mater. Chem.* **18**(42), 5113–5119 (2008).
163. Y. Zhou et al., "Investigation on polymer anode design for flexible polymer solar cells," *Appl. Phys. Lett.* **92**(23), 233308 (2008).
164. M. M. Voigt et al., "Gravure printing for three subsequent solar cell layers of inverted structures on flexible substrates," *Sol. Energy Mater. Sol. Cells* **95**(2), 731–734 (2011).
165. T. Aernouts et al., "Printable anodes for flexible organic solar cell modules," *Thin Solid Films* **451**, 22–25 (2004).
166. F. C. Krebs, S. A. Gevorgyan, and J. Alstrup, "A roll-to-roll process to flexible polymer solar cells: model studies, manufacture and operational stability studies," *J. Mater. Chem.* **19**(30), 5442–5451 (2009).
167. Y. H. Ha et al., "Towards a transparent, highly conductive poly(3,4-ethylenedioxythiophene)," *Adv. Funct. Mater.* **14**(6), 615–622 (2004).
168. J. P. Lock, S. G. Im, and K. K. Gleason, "Oxidative chemical vapor deposition of electrically conducting poly(3,4-ethylenedioxythiophene) films," *Macromolecules* **39**(16), 5326–5329 (2006).
169. Y. Chang, L. Wang, and W. Su, "Polymer solar cells with poly(3,4-ethylenedioxythiophene) as transparent anode," *Org. Electron.* **9**(6), 968–973 (2008).
170. M. V. Fabretto et al., "Polymeric material with metal-like conductivity for next generation organic electronic devices," *Chem. Mater.* **24**(20), 3998–4003 (2012).
171. S. Iijima, "Helical microtubules of graphitic carbon," *Nature* **354**(6348), 56–58 (1991).
172. B. S. Shim et al., "Integration of conductivity transparency, and mechanical strength into highly homogeneous layer-by-layer composites of single-walled carbon nanotubes for optoelectronics," *Chem. Mater.* **19**(23), 5467–5474 (2007).
173. R. H. Baughman, A. A. Zakhidov, and W. A. de Heer, "Carbon nanotubes—the route toward applications," *Science* **297**(5582), 787–792 (2002).
174. Z. Wu et al., "Transparent, conductive carbon nanotube films," *Science* **305**(5688), 1273–1276 (2004).
175. M. Zhang et al., "Strong, transparent, multifunctional, carbon nanotube sheets," *Science* **309**(5738), 1215–1219 (2005).
176. J. L. Bahr et al., "Dissolution of small diameter single-wall carbon nanotubes in organic solvents?," *Chem. Commun.*, 193–194 (2001).
177. J. Chen et al., "Dissolution of full-length single-walled carbon nanotubes," *J. Phys. Chem. B* **105**(13), 2525–2528 (2001).
178. H. T. Ham, Y. S. Choi, and I. J. Chung, "An explanation of dispersion states of single-walled carbon nanotubes in solvents and aqueous surfactant solutions using solubility parameters," *J. Colloid Interface Sci.* **286**(1), 216–223 (2005).
179. S. D. Bergin et al., "Towards solutions of single-walled carbon nanotubes in common solvents," *Adv. Mater.* **20**(10), 1876–1881 (2008).
180. R. Bandyopadhyaya et al., "Stabilization of individual carbon nanotubes in aqueous solutions," *Nano Lett.* **2**(1), 25–28 (2002).
181. M. Zheng et al., "DNA-assisted dispersion and separation of carbon nanotubes," *Nat. Mater.* **2**(5), 338–342 (2003).
182. O. Matarredona et al., "Dispersion of single-walled carbon nanotubes in aqueous solutions of the anionic surfactant NaDDBS," *J. Phys. Chem. B* **107**(48), 13357–13367 (2003).
183. D. S. Hecht et al., "Bioinspired detection of light using a porphyrin-sensitized single-wall nanotube field effect transistor," *Nano Lett.* **6**(9), 2031–2036 (2006).
184. R. Rastogi et al., "Comparative study of carbon nanotube dispersion using surfactants," *J. Colloid Interface Sci.* **328**(2), 421–428 (2008).
185. H.-Z. Geng et al., "Absorption spectroscopy of surfactant-dispersed carbon nanotube film: modulation of electronic structures," *Chem. Phys. Lett.* **455**(4–6), 275–278 (2008).

186. W. Huang et al., "Sonication-assisted functionalization and solubilization of carbon nanotubes," *Nano Lett.* **2**(3), 231–234 (2002).
187. T. P. Tyler et al., "Electronically monodisperse single-walled carbon nanotube thin films as transparent conducting anodes in organic photovoltaic devices," *Adv. Energy Mater.* **1**(5), 785–791 (2011).
188. C. D. Williams et al., "Multiwalled carbon nanotube sheets as transparent electrodes in high brightness organic light-emitting diodes," *Appl. Phys. Lett.* **93**(18), 183506 (2008).
189. R. C. Tenent et al., "Ultrasmooth, large-area, high-uniformity, conductive transparent single-walled-carbon-nanotube films for photovoltaics produced by ultrasonic spraying," *Adv. Mater.* **21**(31), 3210–3216 (2009).
190. Y. I. Song et al., "Flexible transparent conducting single-wall carbon nanotube film with network bridging method," *J. Colloid Interface Sci.* **318**(2), 365–371 (2008).
191. J. Li et al., "Organic light-emitting diodes having carbon nanotube anodes," *Nano Lett.* **6**(11), 2472–2477 (2006).
192. D. Zhang et al., "Transparent, conductive, and flexible carbon nanotube films and their application in organic light-emitting diodes," *Nano Lett.* **6**(9), 1880–1886 (2006).
193. Y. H. Kim et al., "Semi-transparent small molecule organic solar cells with laminated free-standing carbon nanotube top electrodes," *Sol. Energy Mater. Sol. Cells* **96**(1), 244–250 (2012).
194. Y.-M. Chien et al., "A solution processed top emission OLED with transparent carbon nanotube electrodes," *Nanotechnology* **21**(13), 134020 (2010).
195. L. Hu et al., "Flexible organic light-emitting diodes with transparent carbon nanotube electrodes: problems and solutions," *Nanotechnology* **21**(15), 155202 (2010).
196. R. Ulbricht et al., "Transparent carbon nanotube sheets as 3-D charge collectors in organic solar cells," *Sol. Energy Mater. Sol. Cells* **91**(5), 416–419 (2007).
197. C. M. Aguirre et al., "Carbon nanotube sheets as electrodes in organic light-emitting diodes," *Appl. Phys. Lett.* **88**(18), 183104 (2006).
198. Z. Yang et al., "Aligned carbon nanotube sheets for the electrodes of organic solar cells," *Adv. Mater.* **23**(45), 5436–5439 (2011).
199. E. C.-W. Ou et al., "Surface-modified nanotube anodes for high performance organic light-emitting diode," *ACS Nano* **3**(8), 2258–2264 (2009).
200. Q. Zhang et al., "Carbon nanotube mass production: principles and processes," *Chemsuschem* **4**(7), 864–889 (2011).
201. M. F. L. De Volder et al., "Carbon nanotubes: present and future commercial applications," *Science* **339**(6119), 535–539 (2013).
202. M. J. Allen, V. C. Tung, and R. B. Kaner, "Honeycomb carbon: a review of graphene," *Chem. Rev.* **110**(1), 132–145 (2010).
203. M. S. Dresselhaus and P. T. Araujo, "Perspectives on the 2010 Nobel Prize in Physics for Graphene," *ACS Nano* **4**(11), 6297–6302 (2010).
204. A. K. Geim and K. S. Novoselov, "The rise of graphene," *Nat. Mater.* **6**(3), 183–191 (2007).
205. F. Bonaccorso et al., "Graphene photonics and optoelectronics," *Nat. Photonics* **4**(9), 611–622 (2010).
206. R. R. Nair et al., "Fine structure constant defines visual transparency of graphene," *Science* **320**(5881), 1308–1308 (2008).
207. V. C. Tung et al., "High-throughput solution processing of large-scale graphene," *Nat. Nanotechnol.* **4**(1), 25–29 (2009).
208. S. Pang et al., "Graphene as transparent electrode material for organic electronics," *Adv. Mater.* **23**(25), 2779–2795 (2011).
209. M. He et al., "Graphene-based transparent flexible electrodes for polymer solar cells," *J. Mater. Chem.* **22**(46), 24254–24264 (2012).
210. J. Hwang et al., "Multilayered graphene anode for blue phosphorescent organic light emitting diodes," *Appl. Phys. Lett.* **100**(13), 133304 (2012).
211. K. S. Novoselov et al., "Electric field effect in atomically thin carbon films," *Science* **306**(5696), 666–669 (2004).
212. K. S. Novoselov et al., "Two-dimensional gas of massless Dirac fermions in graphene," *Nature* **438**(7065), 197–200 (2005).

213. Y. B. Zhang et al., "Fabrication and electric-field-dependent transport measurements of mesoscopic graphite devices," *Appl. Phys. Lett.* **86**(7), 073104 (2005).
214. L. G. De Arco et al., "Continuous, highly flexible, and transparent graphene films by chemical vapor deposition for organic photovoltaics," *ACS Nano* **4**(5), 2865–2873 (2010).
215. S. Bae et al., "Roll-to-roll production of 30-inch graphene films for transparent electrodes," *Nat. Nanotechnol.* **5**(8), 574–578 (2010).
216. S. Lee et al., "Flexible organic solar cells composed of P3HT:PCBM using chemically doped graphene electrodes," *Nanotechnology* **23**(34), 344013 (2012).
217. Y. Hernandez et al., "High-yield production of graphene by liquid-phase exfoliation of graphite," *Nat. Nanotechnol.* **3**(9), 563–568 (2008).
218. U. Khan et al., "High-concentration solvent exfoliation of graphene," *Small* **6**(7), 864–871 (2010).
219. L. M. Viculis, J. J. Mack, and R. B. Kaner, "A chemical route to carbon nanoscrolls," *Science* **299**(5611), 1361–1361 (2003).
220. C. Valles et al., "Solutions of negatively charged graphene sheets and ribbons," *J. Am. Chem. Soc.* **130**(47), 15802 (2008).
221. H. X. Chang et al., "A transparent, flexible, low-temperature, and solution-processible graphene composite electrode," *Adv. Funct. Mater.* **20**(17), 2893–2902 (2010).
222. G. Eda, G. Fanchini, and M. Chhowalla, "Large-area ultrathin films of reduced graphene oxide as a transparent and flexible electronic material," *Nat. Nanotechnol.* **3**(5), 270–274 (2008).
223. D. Li et al., "Processable aqueous dispersions of graphene nanosheets," *Nat. Nanotechnol.* **3**(2), 101–105 (2008).
224. H. A. Becerril et al., "Evaluation of solution-processed reduced graphene oxide films as transparent conductors," *ACS Nano* **2**(3), 463–470 (2008).
225. Z. Yin et al., "Organic photovoltaic devices using highly flexible reduced graphene oxide films as transparent electrodes," *ACS Nano* **4**(9), 5263–5268 (2010).
226. U. Dettlaff-Weglikowska et al., "Effect of SOCl2 treatment on electrical and mechanical properties of single-wall carbon nanotube networks," *J. Am. Chem. Soc.* **127**(14), 5125–5131 (2005).
227. D. Zhang et al., "Al-TiO2 composite-modified single-layer graphene as an efficient transparent cathode for organic solar cells," *ACS Nano* **7**(2), 1740–1747 (2013).
228. S. De et al., "Silver nanowire networks as flexible, transparent, conducting films: extremely high DC to optical conductivity ratios," *ACS Nano* **3**(7), 1767–1774 (2009).
229. H. Wu et al., "A transparent electrode based on a metal nanotrough network," *Nat. Nanotechnol.* **8**(6), 421–425 (2013).
230. A. R. Rathmell and B. J. Wiley, "The synthesis and coating of long, thin copper nanowires to make flexible, transparent conducting films on plastic substrates," *Adv. Mater.* **23**(41), 4798–4803 (2011).
231. D. Zhang et al., "Synthesis of ultralong copper nanowires for high-performance transparent electrodes," *J. Am. Chem. Soc.* **134**(35), 14283–14286 (2012).
232. T. L. Belenkova et al., "UV induced formation of transparent Au-Ag nanowire mesh film for repairable OLED devices," *J. Mater. Chem.* **22**(45), 24042–24047 (2012).
233. A. Sanchez-Iglesias et al., "Highly transparent and conductive films of densely aligned ultrathin Au nanowire monolayers," *Nano Lett.* **12**(12), 6066–6070 (2012).
234. A. R. Rathmell et al., "Synthesis of oxidation-resistant cupronickel nanowires for transparent conducting nanowire networks," *Nano Lett.* **12**(6), 3193–3199 (2012).
235. J. Krantz et al., "Spray-coated silver nanowires as top electrode layer in semitransparent P3HT:PCBM-based organic solar cell devices," *Adv. Funct. Mater.* **23**(13), 1711–1717 (2013).
236. D. Y. Choi et al., "Annealing-free, flexible silver nanowire-polymer composite electrodes via a continuous two-step spray-coating method," *Nanoscale* **5**(3), 977–983 (2013).
237. T. Stubhan et al., "High fill factor polymer solar cells comprising a transparent, low temperature solution processed doped metal oxide/metal nanowire composite electrode," *Sol. Energy Mater. Sol. Cells* **107**, 248–251 (2012).
238. J.-H. Lee et al., "Brush painting of transparent PEDOT/Ag nanowire/PEDOT multilayer electrodes for flexible organic solar cells," *Sol. Energy Mater. Sol. Cells* **114**, 15–23 (2013).

239. S. M. Bergin et al., "The effect of nanowire length and diameter on the properties of transparent, conducting nanowire films," *Nanoscale* **4**(6), 1996–2004 (2012).
240. E. C. Garnett et al., "Self-limited plasmonic welding of silver nanowire junctions," *Nat. Mater.* **11**(3), 241–249 (2012).
241. T. Tokuno et al., "Fabrication of silver nanowire transparent electrodes at room temperature," *Nano Res.* **4**(12), 1215–1222 (2011).
242. J.-Y. Lee et al., "Semitransparent organic photovoltaic cells with laminated top electrode," *Nano Lett.* **10**(4), 1276–1279 (2010).
243. W. Gaynor et al., "Smooth nanowire/polymer composite transparent electrodes," *Adv. Mater.* **23**(26), 2905–2910 (2011).
244. F. S. F. Morgenstern et al., "Ag-nanowire films coated with ZnO nanoparticles as a transparent electrode for solar cells," *Appl. Phys. Lett.* **99**(18), 183307 (2011).
245. J. Ajuria et al., "Insights on the working principles of flexible and efficient ITO-free organic solar cells based on solution processed Ag nanowire electrodes," *Sol. Energy Mater. Sol. Cells* **102**, 148–152 (2012).
246. W. Gaynor et al., "Color in the corners: ITO-free white OLEDs with angular color stability," *Adv. Mater.* **25**(29), 4006–4013 (2013).
247. C.-C. Chen et al., "Visibly transparent polymer solar cells produced by solution processing," *ACS Nano* **6**(8), 7185–7190 (2012).
248. T. Akter and W. S. Kim, "Reversibly stretchable transparent conductive coatings of spray-deposited silver nanowires," *ACS Appl. Mater. Interfaces* **4**(4), 1855–1859 (2012).
249. M. S. Miller et al., "Silver nanowire/optical adhesive coatings as transparent electrodes for flexible electronics," *ACS Appl. Mater. Interfaces* **5**(20), 10165–10172 (2013).
250. J. L. Elechiguerra et al., "Corrosion at the nanoscale: the case of silver nanowires and nanoparticles," *Chem. Mater.* **17**(24), 6042–6052 (2005).
251. J. Zhao et al., "Electrical breakdown of nanowires," *Nano Lett.* **11**(11), 4647–4651 (2011).
252. D. Zhang et al., "Polymer solar cells with gold nanoclusters decorated multi-layer graphene as transparent electrode," *Appl. Phys. Lett.* **99**(22), 223302 (2011).
253. P. Lin et al., "Semitransparent organic solar cells with hybrid monolayer graphene/metal grid as top electrodes," *Appl. Phys. Lett.* **102**(11), 113303 (2013).

Weiran Cao received his BS degree in materials science from University of Science and Technology of China in 2008 and his PhD degree in materials science and engineering from the University of Florida in 2013. He is currently a postdoctoral researcher in Professor Jiangeng Xue's research group at the University of Florida. His current research work mainly focuses on novel optical designs for organic light-emitting devices and photovoltaic devices.

Jian Li is an associate professor in the School of Materials at Arizona State University. He received his PhD in chemistry from the University of Southern California in 2005. His research interests include design and synthesis of advanced materials for the application in organic semiconductor devices, including organic light-emitting devices, organic photovoltaics, organic memory, and organic thin-film transistors.

Hongzheng Chen is a professor in the Department of Polymer Science & Engineering at Zhejiang University. She received her PhD degree in polymer chemistry and physics from Zhejiang University in 1994. She visited Antwerpen University and Interuniversities Micro-Electronic Center in Belgium during 1999 to 2001 and Stanford University in 2005 and 2007 as a visiting professor. Her research interests focus on organic (organic/inorganic) optoelectronic materials for photovoltaics, photodetection, transistors, and biosensors applications.

Jiangeng Xue is a University of Florida Research Foundation professor and professor of materials science and engineering at the University of Florida. He was also an adjunct professor at Zhejiang University while on sabbatical leave in 2014. He received his PhD in electrical engineering from Princeton University in 2005. His research interests are broadly on the physics and processing of organic and organic-inorganic hybrid electronic materials and their applications in lighting, displays, photovoltaics, photodetection, and circuitry.